NASA TECHNICAL NOTE

NASA TN D-8452

NASA TN D-8452

# ATTITUDE REORIENTATION OF SPACECRAFT BY MEANS OF IMPULSE CONING

*C. William Martz*

*Langley Research Center*
*Hampton, Va. 23665*

NATIONAL AERONAUTICS AND SPACE ADMINISTRATION • WASHINGTON D. C. • AUGUST 1977

| 1. Report No | 2 Government Accession No | 3 Recipient's Catalog No |
|---|---|---|
| NASA TN D-8452 | | |

| 4 Title and Subtitle | 5 Report Date |
|---|---|
| ATTITUDE REORIENTATION OF SPACECRAFT BY MEANS OF IMPULSE CONING | August 1977 |
| | 6 Performing Organization Code |
| 7 Author(s) | 8 Performing Organization Report No |
| C. William Martz | L-11127 |
| | 10 Work Unit No |
| 9 Performing Organization Name and Address | 506-19-13-02 |
| NASA Langley Research Center<br>Hampton, VA 23665 | 11 Contract or Grant No |
| | 13 Type of Report and Period Covered |
| 12 Sponsoring Agency Name and Address | Technical Note |
| National Aeronautics and Space Administration<br>Washington, DC 20546 | 14 Sponsoring Agency Code |

15 Supplementary Notes

16 Abstract

An investigation has been conducted to determine minimum "maneuver costs" for attitude reorientation of spacecraft of all possible inertial distribution over a wide range of maneuver angles by use of the impulse coning method of reorientation. Maneuver cost is proportional to the product of fuel consumed and time expended during a maneuver. Assumptions included impulsive external control torques, rigid-body spacecraft, rest-to-rest maneuvers, and no disturbance torques. Also, coning maneuvers were constrained to have equal initial and final cone angles. Maneuver costs are presented for general reorientations as well as for spin-axis reorientations where final attitude about the spin axis is arbitrary.

| 17 Key Words (Suggested by Author(s)) | 18 Distribution Statement |
|---|---|
| Spacecraft attitude control<br>Spacecraft maneuvering<br>Attitude reorientation<br>Impulse coning<br>Inertia constraints | Unclassified - Unlimited<br><br>Subject Category 13 |

| 19 Security Classif (of this report) | 20 Security Classif (of this page) | 21 No of Pages | 22 Price* |
|---|---|---|---|
| Unclassified | Unclassified | 50 | $4.00 |

* For sale by the National Technical Information Service, Springfield, Virginia 22161

# ATTITUDE REORIENTATION OF SPACECRAFT BY MEANS OF IMPULSE CONING

C. William Martz
Langley Research Center

## SUMMARY

An investigation has been conducted to determine minimum "maneuver costs" for attitude reorientation of spacecraft of all possible inertial distribution over a wide range of maneuver angles by use of the impulse coning method of reorientation. Maneuver cost is proportional to the product of fuel consumed and time expended during a maneuver. Assumptions included impulsive external control torques, rigid-body spacecraft, rest-to-rest maneuvers, and no disturbance torques. Also, coning maneuvers were constrained to have equal initial and final cone angles.

Maneuver costs are presented for general reorientations as well as for spin-axis reorientations where final attitude about the spin axis is arbitrary.

## INTRODUCTION

Impulse coning is a method of attitude reorientation in which impulsive torques are used to initiate and (later) to terminate free precessional motion of a body. Between torque impulses, the spinning body coasts undisturbed through some desired attitude change. Impulse coning has potential application to all maneuvering spacecraft equipped to generate directed external torques.

In past years, attitude reorientation by means of impulse coning has been examined by several authors (refs. 1 to 4). Reference 1 suggests that large-angle reorientations of axisymmetric bodies be accomplished with a series of "small-angle" precessional motions. Reference 2 presents a two-impulse coning scheme for large-angle spin-axis reorientations of axisymmetric bodies. Spin-axis or pointing-axis reorientations can be defined as general reorientations with final attitude about the spin or pointing axis arbitrary. Reference 3 extends the spin-axis reorientations of reference 2 to asymmetric bodies. However, precession angle is restricted to 180° and spin-axis inertia must be larger than inertias about transverse axes. Reference 4 introduces a statistical "average cost" for general reorientations over a specified maneuver-angle range and favorably compares two-impulse coning costs with costs of other reorientation methods. Results are limited to elongated axisymmetric bodies, however.

The present paper extends previous results to include two-impulse coning costs for general reorientations of axisymmetric foreshortened bodies. Also, two-impulse coning costs are obtained for spin-axis reorientations of asymmetric bodies of all possible inertial distribution. Finally, maneuver costs are

determined for general reorientations of asymmetric bodies. In this category, maneuvers consist of a coning motion followed by an impulsive spin maneuver to obtain the desired spin attitude.

In the present investigation, reaction thrusters are assumed to initiate and terminate all coning motions with impulsive torques of negligible duration. Other assumptions include rigid-body spacecraft, lack of disturbance torques, and rest-to-rest maneuvers (zero initial and final attitude rates).

The product of total maneuver impulse (proportional to fuel consumed) and total maneuver time is determined for the various solution paths available for each maneuver. This product is then nondimensionalized by spacecraft inertia about the intermediate principal axis and is referred to as the cost function for that maneuver. Since total impulse and maneuver time are inversely proportional for impulsive maneuvers, results are independent of each of these quantities. The desired or optimal solution is defined as the solution associated with the smallest cost function for each maneuver. Since it was assumed that all reorientations within a given range of maneuver angle are equally probable, optimal cost functions for a large number of statistically representative reorientations within a given maneuver range were averaged to represent reorientation costs for that maneuver range. Maneuver ranges of 0.00873, $\pi/4$, $\pi/2$, and $\pi$ radians were used.

## SYMBOLS

| | |
|---|---|
| F | nondimensional asymmetry factor defined by equation (17) |
| FLAG | indicator of nutation class (see eq. (12)) |
| H | total angular momentum, defined as positive for $\dot{\psi} > 0$ and negative for $\dot{\psi} < 0$ |
| $H_x, H_y, H_z$ | angular momentum components along x-,y-,z-axes, respectively |
| $H_{xy}$ | angular momentum in transverse plane, $\sqrt{H_x^2 + H_y^2}$ |
| I | transverse inertia for roll-symmetric bodies |
| $I_x, I_y, I_z$ | principal body inertias about x-,y-,z-axes, respectively; $I_y$ is intermediate moment of inertia |
| m | mass element |
| n | = 0, 1, 2, 3, . . . |
| $Q_p$ | product of impulse and time for thruster prepositioning |
| $Q_s$ | product of total impulse and total time divided by $I_y$ for spin maneuver (see eq. (38)) |

$Q_2$ product of total impulse and total time divided by $I_y$ for coning maneuver (fixed thrusters)

$Q_{2,A}$ axial component of $Q_2$ (see eqs. 36))

$Q_{2,T}$ transverse component of $Q_2$ (see eqs. (36))

$Q_{2,swivel}$ product of total impulse and total time divided by $I_y$ for coning maneuver (thrusters on spin axis swiveled)

$Q_3$ product of total impulse and total time divided by $I_y$ for three-impulse coning-spin maneuver

$R_1,R_2,R_3$ sequential Euler angle rotations about z-,y-,z-axes, respectively, relating body axes before and after reorientation (see fig. 4), $R_2$ also referred to as maneuver angle

$R_{2,max}$ maneuver range, radians; $0 \leqq R_2 \leqq R_{2,max}$

sgn ( ) sign of quantity

T kinetic energy (see eq. (23))

t time, sec

$t_f$ coning maneuver time, sec

$t_s$ spin maneuver time, sec

X,Y,Z inertial coordinate axis system

x,y,z body principal coordinate axis system; unless otherwise specified, z is spin axis

$x_d'$ $x_d$-axis translated from mass center along $z_f$-axis

$x_f'$ $x_f$-axis translated from mass center along $z_f$-axis

$x_o'$ $x_o$-axis translated from mass center along $z_o$-axis

y' y-axis translated from mass center along $z_o$-axis after $R_1$ rotation

$\Delta\phi$ change in spin angle during coning, $\phi_f - \phi_o$

$\varepsilon$ error in spin angle at termination of coning maneuver (see fig. 4)

$\theta_m$ extremum value of $\theta$ (see text following eq. (19))

$\psi,\theta,\phi$ rotation sequence of Euler angles about x-,y-,z-axes, respectively, relating inertial and body coordinate axis systems

$\dot{\psi},\dot{\theta},\dot{\phi}$ Euler rates

$\psi_s$ "spherical" values of $\psi$ defined by equation (6)

$\omega_x,\omega_y,\omega_z$ body rates about x-,y-,z-axes, respectively

Subscripts:

av average value (with respect to time) during maneuver

d desired value

f value at conclusion of coning maneuver

max maximum value

min minimum value

o value at start of coning maneuver

## ANALYSIS

### Equations of Motion

Two coordinate axis systems used in the analysis of the impulse coning method of attitude reorientation are illustrated in figure 1. The body principal axis system x,y,z is related to an inertial axis system X,Y,Z by an Euler rotation sequence $\psi,\theta,\phi$ about body axes z,y,z, respectively. Note that $\dot{\psi}$ and Z are chosen to be in the same direction as the total angular momentum H. Angular momentum H is established for each reorientation maneuver by the initial torque impulse of the thrusters. Reaction thrusters are assumed to be fixed along the x,y,z body axes to produce torques about the y-,z-,x-axes, respectively. Without loss of generality, $\theta$ is restricted to $0 < \theta < \pi/2$.

From figure 1(a), the relationships between inertial rates and body rates $\omega_x$, $\omega_y$, and $\omega_z$ are

$$\left.\begin{aligned} \dot{\psi} &= \frac{\omega_y \sin\phi - \omega_x \cos\phi}{\sin\theta} \\ \dot{\theta} &= \omega_y \cos\phi + \omega_x \sin\phi \\ \dot{\phi} &= \omega_z - \dot{\psi}\cos\theta \end{aligned}\right\} \tag{1}$$

The angular momenta along the body axes (from fig. 1(b)) are

$$\left.\begin{aligned} H \cos\theta &= I_z\omega_z \\ H \sin\theta \sin\phi &= I_y\omega_y \\ -H \sin\theta \cos\phi &= I_x\omega_x \end{aligned}\right\} \tag{2}$$

Combining equations (1) and (2) yields the Euler rate equations governing the coning motion, which are

$$\left.\begin{aligned} \dot{\psi} &= H\left(\frac{\sin^2\phi}{I_y} + \frac{\cos^2\phi}{I_x}\right) \\ \dot{\theta} &= H\left(\frac{1}{I_y} - \frac{1}{I_x}\right)\sin\theta \sin\phi \cos\phi \\ \dot{\phi} &= H\frac{\cos\theta}{I_z} - \dot{\psi}\cos\theta \end{aligned}\right\} \tag{3}$$

## Axisymmetric Bodies

The Euler rate equations (eqs. (3)) are easily integrated for axisymmetric ($I_x = I_y = I$) bodies with the result for $\psi_o = 0$ expressed as

$$\psi = \frac{H}{I}t \qquad \text{and} \qquad \psi_f = \frac{H}{I}t_f$$

$$\theta = \theta_o = \theta_f = \text{Constant}$$

$$\phi = \phi_o + \psi \cos\theta_o\left(\frac{I}{I_z} - 1\right)$$

and

$$\Delta\phi = \phi_f - \phi_o = \psi_f \cos\theta_o\left(\frac{I}{I_z} - 1\right) \tag{4}$$

This solution is the free precessional motion of a spinning body as illustrated in figure 2. The specified initial and final locations of the body $z$ (spin) axis are elements of a space cone connected by a coning or precession circle. The total angular momentum $H$ and the $Z$ inertial axis are coincident with the cone axis.

An impulse coning maneuver is performed as follows: The body, initially at rest, is acted upon by an external control torque impulse of negligible duration which causes it to spin about its z-axis and precess about the Z-axis. When the spin axis reaches the desired final location, a second external torque impulse terminates the precessional motion. If the body attitude about the spin axis $\phi$ is as desired, the second impulse also terminates the spinning motion. Otherwise, the second impulse will include a component along the spin axis to initiate a corrective spin maneuver which is terminated by a third impulse.

The axial and transverse momentum components generated by the initial impulse are labeled $H_{z,o}$ and $H_{xy,o}$ in figure 2. Also, the momentum components which terminate the motion are shown as $H_{z,f}$ and $H_{xy,f}$. The initial body-axis system $x_o,y_o,z_o$ is included to illustrate the orientation of $H$ in body coordinates.

It should be mentioned that candidate coning solutions to equations (3) must include negative as well as positive precession rates and spin rates. For example, the two pairs of alternative paths illustrated in figure 3 are similar geometrically but differ in the sign of $\dot{\psi}$ and $\dot{\phi}$ and therefore have unlike final spin attitudes.

The spherical geometry of a generalized reorientation maneuver $R_1,R_2,R_3$ is shown in figure 4. By definition, $R_1,R_2,R_3$ is any specified set of sequential Euler angle rotations about the $z,y,z$ body axes, respectively, which reorient the body from its initial attitude to some final desired attitude.

Parameter relationships for the coning motion can be determined from the geometry of figure 4. The oblique spherical triangle with sides $\theta_o$, $R_2$, and $\theta_f$ is bisected into two right spherical triangles with mirror symmetry. From the leftmost triangle of figure 4(a)

$$\sin \theta_o = \left| \frac{\sin (R_2/2)}{\sin (\psi_f/2)} \right| \tag{5}$$

and

$$\sin (\psi_s/2) = \frac{\tan (R_2/2)}{\tan \theta_o} \operatorname{sgn} \dot{\psi} \tag{6}$$

where $\operatorname{sgn} \dot{\psi}$ is used to control the sign of $\psi_s$. At the start of coning (see fig. 4)

$$\phi_o - \frac{\psi_s}{2} + R_1 = \frac{\pi}{2}(2 - \operatorname{sgn} \dot{\psi}) \tag{7}$$

At the end of coning

$$\phi_f + \frac{\psi_s}{2} + \varepsilon - R_3 = \frac{\pi}{2}(\operatorname{sgn} \dot{\psi}) \tag{8}$$

Equations (7) and (8) are combined to yield the following equation for the error in spin angle:

$$\varepsilon = R_1 + R_3 - \psi_s - \Delta\phi + \pi(\operatorname{sgn} \dot{\psi} - 1)$$

and because of its cyclic nature, $\varepsilon$ can be written

$$\varepsilon = R_1 + R_3 - \psi_s - \Delta\phi \pm 2\pi n \qquad (n = 0, 1, 2, \ldots) \tag{9}$$

where the value of $n$ is adjusted to minimize the absolute value of $\varepsilon$ to eliminate unnecessary maneuver costs.

Equations (5), (6), (4), (7), and (9) govern the coning solution and relate the variables $\psi_f$, $\theta$, $\psi_s$, $\Delta\phi$, $\phi_o$, and $\varepsilon$, for a given maneuver $(R_1,R_2,R_3)$ and inertial distribution $(I_x = I_y \neq I_z)$. Also, these variables and constants combine to generate a cost function for each maneuver as reported in the section entitled "Reorientation Costs." Because the solution is under-defined (more variables than independent equations) it was necessary to perform a trial-and-error search (search variable $\psi_f$) to determine the solution with the smallest cost function for each maneuver. All such solutions were found to occur at $\varepsilon = 0$. That is, two-impulse coning not only is sufficient for all reorientations of axisymmetric bodies but also results in minimum reorientation costs.

## Asymmetric Bodies

For asymmetric bodies $\left(I_x \lessgtr I_y \lessgtr I_z\right)$, the Euler rate equations (eqs. (3)) are nonlinear, and analytical solutions are not available except in the form of elliptic functions. A more useful approach is the application of Poinsot's construction which is presented in reference 5. This method qualitatively

analyzes the free motions of rigid bodies and indicates that the motion of asymmetric bodies is similar in many ways to that of symmetric bodies. A notable exception is the nutational or nodding motions of the z-axis as it precesses about the momentum vector. Thus, for asymmetric bodies, $\theta$ is oscillatory as are the time histories of the Euler rates.

In order to exploit the energy-momentum relationships of the Poinsot method and determine quantitative information regarding the free motion of asymmetric bodies, it was decided to restrict solutions to the class for which $\theta_f = \theta_o$. This restriction not only furnished an additional equation in $\theta$, but imposed a symmetry of motion on all solutions which in turn constrained $\phi$ and eliminated the need for trial-and-error solutions.

Figure 2 illustrates nutational motion during the coning maneuver by the curves labeled "Inner path" and "Outer path." That is, there are two separate solutions for each maneuver which satisfy all initial conditions as well as the imposed terminal condition $\theta_f = \theta_o$. These solutions are shown quantitatively in figure 5 which presents normalized $\theta$-$\psi$ trajectories obtained by numerically integrating equations (3) for an example maneuver. Because of the terminal condition ($\theta_f = \theta_o$), all such trajectories are characterized by a symmetry of motion about the midtrajectory point. It can be shown with equations (3) that spinning motion associated with inward nutation is antisymmetric about the midtrajectory point $\phi = 0 \pm \pi n$; this leads to the following roll-constraint equation for inward nutation:

$$\phi_f + \phi_o = 0 \pm 2\pi n \qquad (n = 0, 1, 2, \ldots) \qquad (10)$$

The last term of the two equations in the preceding sentence derives from the symmetry of the inertia ellipsoid (ref. 5) about the body spin axis and the periodic nature of $\phi$. If $\phi_o$ is changed by increments of $\pm 2\pi$, $\pm 4\pi$, $\pm 6\pi$, etc., before the initial coning impulse, the coning motion will be unchanged. Also, $\phi_o$ can be changed by increments of $\pm\pi$, $\pm 3\pi$, $\pm 5\pi$, etc., without changing the coning motion providing the transverse impulse torques are applied in the opposite direction. These alternatives are implied by the last term of equation (10).

Referring again to figure 5, the path labeled "Outward nutation" is part of a trajectory set for which the spinning motion is antisymmetrically centered about $\phi = \pi/2 \pm \pi n$ causing the roll-constraint equation for outward nutation to be

$$\phi_f + \phi_o = \pi \pm 2\pi n \qquad (n = 0, 1, 2, \ldots) \qquad (11)$$

The last term is included for reasons just mentioned in connection with equation (10). For manipulative convenience, equations (10) and (11) are combined into a single constraint equation which is

$$\phi_f + \phi_o = \pi(\text{FLAG}) \pm 2\pi n \qquad (n = 0, 1, 2, \ldots) \tag{12}$$

where FLAG = 0 for inward nutation and FLAG = 1 for outward nutation. This roll constraint precludes two-impulse coning reorientations of asymmetric bodies for the condition $\theta_f = \theta_o$ except for a few maneuvers which satisfy the following combination of equations (7), (8), and (12) for $\varepsilon = 0 \pm 2\pi n$:

$$R_3 - R_1 = \pi(\text{FLAG} - 1 \pm 2n) \qquad (n = 0, 1, 2, \ldots) \tag{13}$$

All other coning reorientations of asymmetric bodies require a follow-up spin correction maneuver.

Another relationship pertinent to the coning motions of asymmetric bodies concerns precession time and is written

$$t_f = \frac{\psi_f - \psi_o}{\dot{\psi}_{av}} \tag{14}$$

where $\psi_o = 0$ and $\dot{\psi}_{av}$ is determined by integrating the first of equations (3) to obtain

$$\dot{\psi}_{av} = H\left(\frac{\cos^2 \phi}{I_x} + \frac{\sin^2 \phi}{I_y}\right)_{av} \approx \frac{H}{\Delta\phi}\int_{\phi_o}^{\phi_f}\left(\frac{\cos^2 \phi}{I_x} + \frac{\sin^2 \phi}{I_y}\right) d\phi$$

or

$$\dot{\psi}_{av} \approx H\left[\frac{I_x + I_y}{2I_xI_y} + \frac{I_y - I_x}{2I_xI_y}\,\frac{\sin(2\phi_f) - \sin(2\phi_o)}{2(\Delta\phi)}\right] \tag{15}$$

Equation (15) represents the average $\dot{\psi}$ with respect to $\phi$ over the coning maneuver and thus an approximation to the average $\dot{\psi}$ with respect to time required by equation (14). However, the error of this approximation was found to be negligible for the maneuvers of the present paper. For example, this error is less than one part in ten thousand for the trajectories of figure 5. Combining equations (12), (14), and (15) and simplifying yield

$$t_f = \frac{\psi_f I_x}{H(F)} \tag{16}$$

where

$$F = \frac{I_x + I_y}{2I_y} + \left[1 - 2(\mathrm{FLAG})\right]\frac{I_y - I_x}{2I_y}\,\frac{\sin(\Delta\phi)}{\Delta\phi} \tag{17}$$

An independent source for $\Delta\phi$ is obtained by integrating the third of equations (3) to yield

$$\Delta\phi = \int_0^{t_f} \dot{\phi}\, dt = \int_0^{t_f} \left(\frac{H \cos\theta}{I_z} - \dot{\psi}\cos\theta\right) dt$$

Replacing $\cos\theta$ with its average value during the coning maneuver and integrating give

$$\Delta\phi = \frac{Ht_f(\cos\theta)_{av}}{I_z} - \psi_f(\cos\theta)_{av} \tag{18}$$

The last term is an approximation to the original integral and is not accurate for maneuvers having large variations in $\theta$. However, $\theta$ variations as monitored for optimum reorientations were small without exception and, by using the following approximation for $(\cos\theta)_{av}$,

$$(\cos\theta)_{av} \approx \frac{\int_{\theta_o}^{\theta_f} \cos\theta\, d\theta}{\theta_f - \theta_o} = \frac{2\int_{\theta_o}^{\theta_m} \cos\theta\, d\theta}{2(\theta_m - \theta_o)} = \frac{\sin\theta_m - \sin\theta_o}{\theta_m - \theta_o} \tag{19}$$

equation (18) has been found to compare closely with numerically integrated results. In equation (19), $\theta_m$ is the limiting or extremum value of $\theta$ as given by equation (31) or (32) or (33) or (34), depending upon the polhode axis and whether the nutation is inward or outward, as explained in the section entitled "Nutational Motion Limits."

Combining equations (16), (18), and (19) gives

$$\Delta\phi = \psi_f\left(\frac{\sin\theta_m - \sin\theta_o}{\theta_m - \theta_o}\right)\left(\frac{I_x/I_z}{F} - 1\right) \tag{20}$$

Equations (12), (7), (6), (31) or (32), (5), (20), and (9), which govern variables $\phi_o$, $\psi_s$, $\theta_o$, $\theta_m$, $\psi_f$, $\Delta\phi$, and $\varepsilon$, respectively, were solved iteratively in the order specified by the Newton-Raphson method for each given maneuver and inertial distribution. The amplitude of $\Delta\phi$ used to start the iterative solution was set initially at 0.000001 and successively increased to 0.5, 1, and 2 until convergence occurred. Four separate solution paths (one for each of the $\theta_m$ values referred to in connection with eq. (19)) were available for both positive and negative precession rates - a total of eight possible solutions for each reorientation. All such solutions were determined and the one associated with minimum maneuver costs was retained for computing the "average cost" of reorientations presented for each maneuver range. The listing and documentation of computer program ASYMCON, used to determine these solutions, is presented in appendix A.

## Polhode Axes

Poinsot's geometric solution, described in references 5 and 6, equates the free rotational motion of a rigid body to the motion of the "ellipsoid of inertia" for that body as it rolls on the "invariable plane." The point of contact between these two surfaces traces out a "polhode" curve on the ellipsoid of inertia. The axis surrounded by the polhode curve, or "polhode axis," is the body axis which precesses about the momentum vector during a coning maneuver. The polhode axis, which can be an axis of minimum moment of inertia or an axis of maximum moment of inertia but not an axis of intermediate moment of inertia, is determined by the initial motion and inertial distribution of the body.

It is necessary to determine the polhode axis for each coning maneuver before the angular limits of the nutational motion can be determined. Consider first the class of bodies for which

$$I_x > I_y > I_z$$

Reference 6 indicates that the condition for polhode about the z-axis is

$$I_y > \frac{H^2}{2T} > I_z \tag{21}$$

where $H^2$, or $(\text{Momentum})^2$, is expressed

$$H^2 = (I_x\omega_x)^2 + (I_y\omega_y)^2 + (I_z\omega_z)^2 \tag{22}$$

and 2T, or 2(Kinetic energy), is expressed

$$2T = I_x\omega_x^2 + I_y\omega_y^2 + I_z\omega_z^2 \tag{23}$$

Equations (22) and (23), with body rates substituted from equations (2), are combined with that part of inequality (21) concerned with intermediate inertia $I_y$, and the condition becomes, for polhode about the z-axis,

$$\tan^2\theta\ \cos^2\theta < \frac{I_x(I_y - I_z)}{I_z(I_x - I_y)} \qquad (I_x > I_y > I_z)$$

where $\theta$ and $\phi$ are chosen to be the initial conditions $\theta_o$ and $\phi_o$. The condition for polhode about the x-axis is

$$I_x > \frac{H^2}{2T} > I_y \tag{24}$$

Again the momentum and energy expressions, with body rates from equations (2), are substituted into the part of inequality (24) involving $I_y$, and the condition becomes, for polhode about the x-axis,

$$\tan^2\theta\ \cos^2\phi > \frac{I_x(I_y - I_z)}{I_z(I_x - I_y)} \qquad (I_x > I_y > I_z)$$

Now consider the remaining asymmetric bodies which are in the class

$$I_x < I_y < I_z$$

The condition for polhode about the z-axis is

$$I_z > \frac{H^2}{2T} > I_y \tag{25}$$

Substituting the momentum and energy expressions and body rates into the $I_y$ part of inequality (25) results in the condition

$$\tan^2\theta\ \cos^2\phi < \frac{I_x(I_y - I_z)}{I_z(I_x - I_y)} \qquad (I_x < I_y < I_z)$$

for polhode about the z-axis. Finally, the condition for polhode about the x-axis is

$$I_y > \frac{H^2}{2T} > I_x \tag{26}$$

Again, substituting the momentum and energy expressions and body rates into the part of polhode condition (26) involving $I_y$ yields the condition for polhode about the x-axis

$$\tan^2 \theta \cos^2 \phi > \frac{I_x(I_y - I_z)}{I_z(I_x - I_y)} \qquad (I_x < I_y < I_z)$$

In summary, polhode is about the x-axis if

$$\tan^2 \theta \cos^2 \phi > \frac{I_x(I_y - I_z)}{I_z(I_x - I_y)} \tag{27}$$

Conversely, polhode is about the z-axis if

$$\tan^2 \theta \cos^2 \phi < \frac{I_x(I_y - I_z)}{I_z(I_x - I_y)} \tag{28}$$

## Nutational Motion Limits

As the spin axis of a rigid asymmetric body precesses about the angular momentum vector in free rotational motion, a nutation or nodding of the axis occurs which causes the half-cone angle $\theta$ to oscillate between some maximum and minimum values. These limiting values are derived in reference 5 and presented along with an analysis of the motion. The limits are needed in the present investigation to determine the mean value of the half-cone angle during the coning maneuver for use with equation (19).

Reference 5 shows that for a polhode about the z-axis and either $I_x \geqq I_y > I_z$ or $I_x \leqq I_y < I_z$

$$\tan^2 \theta_{max} = \frac{I_y\left(H^2 - 2TI_z\right)}{I_z\left(2TI_y - H^2\right)} \tag{29}$$

and

$$\tan^2 \theta_{min} = \frac{I_x\left(H^2 - 2TI_z\right)}{I_z\left(2TI_x - H^2\right)} \tag{30}$$

where $\theta_{max}$ and $\theta_{min}$ are the limiting values of $\theta$ over a full precession cycle. The coning maneuvers of the present paper use only a small part of this cycle, however. Thus, only $\theta_{max}$ is needed for outward nutations and only $\theta_{min}$ is needed for inward nutations.

These motion limits can be expressed as a function of inertial distribution and Euler angles by substitutions for the momentum and energy (eqs. (22) and (23)) and the body rate (eqs. (2)). The following equations result for polhode about the z-axis:

$$\theta_{max} = \tan^{-1}\left[\sqrt{\frac{I_y(I_z - I_x) + I_x(I_z - I_y)\tan^2 \phi}{I_z(I_x - I_y) + I_x(I_z - I_y)/(\tan^2 \theta \cos^2 \phi)}}\right] \tag{31}$$

and

$$\theta_{min} = \tan^{-1}\left[\sqrt{\frac{I_y(I_z - I_x) + I_x(I_z - I_y)\tan^2 \phi}{I_z(I_y - I_x)\tan^2 \phi + I_y(I_z - I_x)/(\tan^2 \theta \cos^2 \phi)}}\right] \tag{32}$$

where $\phi$ and $\theta$ are chosen to be evaluated at the instant coning starts.

Thus far, limits have been determined only for motions characterized by polhodes about the z-axis. Consider now the alternative maneuvers with polhodes about the x-axis. The motion-limit formulas of reference 5 can be related to $\theta_{max}$ and $\theta_{min}$ only when $\theta$ is measured from the polhode axis. Rather than rederive the equations of motion based on $\theta$ being measured from the x-axis, a two-step alternative was employed to use the existing equations of motion for maneuvers having polhodes about the x-axis. The first step is to interchange the values of $I_x$ and $I_z$. The second step is to replace the original Euler rotations about the z-, y-, and z-axes with a newly generated set of Euler rotations about the -x-, y-, and -x-axes designed to produce the identical body reorientation. The new set of Euler angles was determined by the method of reference 7 and implemented in program ASYMCON of appendix A. With these changes, the coning geometry is transferred, in effect, from polhode about the z-axis to polhode about the x-axis.

Reference 5 indicates that for a polhode about the x-axis and for either $I_x < I_y \leqq I_z$ or $I_x > I_y \geqq I_z$, the limiting values of $\theta$ can be determined from equations (29) and (30) with substitutions of equations (22), (23), and (2), providing $I_x$ and $I_y$ are interchanged. The resulting motion limits for polhode about the x-axis are

$$\theta_{max} = \tan^{-1}\sqrt{\frac{I_z(I_y - I_x)\tan^2\phi + I_y(I_z - I_x)}{I_z(I_y - I_x)/(\tan^2\theta\cos^2\phi) + I_x(I_y - I_z)}} \tag{33}$$

and

$$\theta_{min} = \tan^{-1}\sqrt{\frac{I_z(I_y - I_x)\tan^2\phi + I_y(I_z - I_x)}{I_y(I_z - I_x)/(\tan^2\theta\cos^2\phi) + I_x(I_z - I_y)\tan^2\phi}} \tag{34}$$

where $\theta$ and $\phi$ again are chosen to be evaluated at the instant coning starts. Note that these motion limits for polhode about the x-axis can be obtained from equations (31) and (32) (motion limits for polhode about the z-axis) simply by interchanging $I_x$ and $I_z$.

## REORIENTATION COSTS

As mentioned in the Introduction, a cost function equal to the product of total maneuver impulse (proportional to fuel consumed) and total maneuver time, nondimensionalized by spacecraft inertia about the intermediate principal axis, is determined for the various solution paths available for each maneuver. The desired or optimum path is defined as the path associated with the smallest cost function for each coning maneuver. Since total impulse and maneuver time are inversely proportional for impulsive maneuvers, results are independent of each of these quantities.

It is assumed that all reorientations within a given maneuver range $R_{2,max}$ are equally probable. Therefore, reorientation costs were sampled within each given maneuver range by systematically computing optimum cost functions for combinations of $R_1$, $R_2$, and $R_3$ at equally spaced intervals throughout the sample space limits $-\pi \leqq R_1 < \pi$, $0 \leqq R_2 \leqq R_{2,max}$, and $-\pi \leqq R_3 \leqq \pi$ where $R_{2,max} = 0.0087$, $\pi/4$, $\pi/2$, and $\pi$. These optimum cost functions were then weighed (according to likelihood of occurrence) and averaged as follows:

$$\text{Average cost} = \frac{\Sigma(\text{Optimum cost} \times \sin R_2)}{\Sigma(\sin R_2)}$$

In addition, the standard deviation of the optimum cost functions was determined with the relationship

$$\text{Standard deviation} = \sqrt{\frac{\Sigma\left[(\text{Optimum cost})^2 \times \sin R_2\right]}{\Sigma(\sin R_2)} - (\text{Average cost})^2}$$

## Cost Equations

The impulse (and thus momentum) required to initiate and terminate coning maneuvers has two components (see fig. 2): the transverse component

$$H_{xy,o} = H_{xy,f} = H \sin \theta_o$$

and the axial component

$$H_{z,o} = H_{z,f} = H \cos \theta_o$$

For reaction thrusters fixed along the x, y, and z body axes to produce torques about the y-, z-, and x-axes, respectively, the cost function (Total impulse × Total time)/$I_y$ for the two-impulse coning maneuver is

$$Q_2 = Q_{2,T} + Q_{2,A} \tag{35}$$

where the transverse and axial components are

$$\left.\begin{aligned} Q_{2,T} &= \frac{|H| \sin (\theta_o)t_f}{I_y}\left(|\sin \phi_o| + |\cos \phi_o| + |\sin \phi_f| + |\cos \phi_f|\right) \\ Q_{2,A} &= \frac{2|H| \cos (\theta_o)t_f}{I_y} \end{aligned}\right\} \tag{36}$$

If the thruster pair fixed on the spin axis to produce torques about the x-axis is allowed to swivel about the spin axis, the components of $Q_{2,T}$ can be minimized (reduced about 21 percent on the average) at the expense of a relatively small thruster prepositioning term $Q_p$ with the result expressed as

$$Q_{2,\text{swivel}} = \frac{|2H(\sin \theta_o)t_f + 2H(\cos \theta_o)t_f|}{I_y} + Q_p$$

Because the thruster prepositioning term introduces variables which make cost comparisons between swiveled and fixed thrusters somewhat arbitrary, maneuver costs for swiveled thrusters will not be pursued beyond this equation.

For axisymmetric bodies ($I_x = I_y = I$), the precession time $t_f$ is determined from the equation

$$t_f = \frac{\psi_f - \psi_o}{\dot{\psi}_{av}} = \frac{\psi_f - 0}{H/I}$$

and the cost function becomes

$$Q_2 = |\psi_f| \sin \theta_o \left(|\sin \phi_o| + |\cos \phi_o| + |\sin \phi_f| + |\cos \phi_f|\right) + 2|\psi_f| \cos \theta_o \tag{37}$$

Turning now to asymmetric $\left(I_x \lesseqgtr I_y \lesseqgtr I_z\right)$ bodies, it is necessary because of the assumed terminal constraint $\theta_f = \theta_o$ to combine the coning maneuver with a final spin maneuver to attain the desired roll attitude. The resulting three-impulse cost function is

$$Q_3 = \frac{\text{Total impulse} \times \text{Total time}}{I_y} = \left(\frac{Q_2}{t_f} + \frac{Q_s}{t_s}\right)(t_f + t_s)$$

where the cost function for the spin maneuver is

$$Q_s = \frac{2|\varepsilon| I_z}{I_y} - 0.5\left(1 + \frac{|\psi_f \varepsilon|}{\psi_f \varepsilon}\right) Q_{2,A}\left(\frac{t_s}{t_f}\right) \tag{38}$$

The last term of $Q_s$ derives from the fact that axial momentum at termination of coning can be used to reduce the momentum required for the spin correction maneuver provided the momenta are in the same direction.

From equations (36) and (16),

$$\left.\begin{aligned} Q_{2,A} &= \frac{2I_x|\psi_f| \cos \theta_o}{I_y F} \\ Q_{2,T} &= \frac{I_x|\psi_f| \sin \theta_o}{I_y F}\left(|\sin \phi_o| + |\cos \phi_o| + |\sin \phi_f| + |\cos \phi_f|\right) \end{aligned}\right\} \tag{39}$$

For minimum $Q_3$

$$\left.\begin{aligned} \frac{dQ_3}{d(t_s/t_f)} &= 0 = Q_2 - \frac{2|\varepsilon| I_z}{I_y}\left(\frac{t_f}{t_s}\right)^2 - 0.5\left(1 + \frac{|\psi_f\varepsilon|}{\psi_f\varepsilon}\right)Q_{2,A} \\ \frac{d^2Q_3}{d(t_s/t_f)^2} &= \frac{2|\varepsilon| I_z}{I_y}\left(\frac{t_f}{t_s}\right)^3 > 0 \end{aligned}\right\} \tag{40}$$

The time constraint introduced by equations (40) causes the minimum three-impulse cost function to be

$$Q_{3,min} = \frac{2|\varepsilon| I_z}{I_y}\left(1 + \frac{t_f}{t_s}\right)^2 \tag{41}$$

where for $\psi_f\varepsilon < 0$,

$$\frac{t_f}{t_s} = \sqrt{\frac{Q_{2,T} + Q_{2,A}}{2|\varepsilon| I_z/I_y}} \tag{42}$$

and for $\psi_f\varepsilon > 0$,

$$\frac{t_f}{t_s} = \sqrt{\frac{Q_{2,T}}{2|\varepsilon| I_z/I_y}} \tag{43a}$$

or

$$\frac{t_f}{t_s} = \frac{Q_{2,A}}{2|\varepsilon| I_z/I_y} \tag{43b}$$

whichever is larger. This singularity in $t_f/t_s$ is caused by the minimum cost requirement that the spin correction momentum be larger than the axial momentum at the end of coning.

For application of equation (41), the iterative solution discussed just subsequent to equation (20) was used with equations (38), (39), and (42) or (43).

## Spin-Axis Reorientation Costs

All spin-axis reorientations were accomplished with two-impulse coning maneuvers. For roll-symmetric bodies, the cost function is given by equation (37). For asymmetric bodies, the cost function is specified by equations (35) and (39).

# RESULTS

The results of this investigation are primarily the costs of reorientation by the impulse coning method. These are presented in the form of average cost as functions of $1 - I_z/I_y$ and $R_{2,max}$ for bodies of all possible inertial distribution which are identified in appendix B and presented in figure 6. Results for general reorientations are presented first, followed by results for spin-axis reorientations and certain cost comparisons. Spin-axis reorientations are defined as reorientations with final attitude about the spin axis arbitrary.

Figure 7 shows the effect of inertial distribution on average cost of reorientation for maneuver ranges of $\pi$, $\pi/2$, $\pi/4$, and 0.00873 radians. The lowest curve ($I_x \equiv I_y$) of each plot represents the family of axisymmetric bodies. This curve contains minimal two-impulse coning costs and is seen to be in agreement with similar results available from reference 4 for elongated bodies with $R_{2,max} = \pi$. The average cost of maneuvering is seen to decrease as bodies become less foreshortened or more elongated.

The remaining curves in figure 7 are for asymmetric bodies and represent coning trajectories restricted to the terminal condition $\theta_f = \theta_o$. With few exceptions, these results for asymmetric bodies do not share the lower maneuver costs of axisymmetric bodies. Comparable reorientation costs for asymmetric bodies are greater for two reasons. First, the nutational motion prevents many potentially low-cost trajectories from meeting the terminal condition $\theta_f = \theta_o$. Second, as mentioned in connection with equation (13), almost all coning trajectories of asymmetric bodies are unable to satisfy the roll-constraint equation without a follow-up spin correction maneuver and increased costs. These reasons are applicable to asymmetries as small as one part in a million as indicated by a comparison of the $I_x \equiv I_y$ and $I_x \approx I_y$ curves. In this comparison, the abrupt jump in maneuver costs due to the slightest asymmetry is real but, in a practical sense, could be attributed to excessive accuracy requirements on the $\theta$ and $\phi$ terminal constraints. In other words, if these terminal constraints were relaxed to $x$ parts error per million parts, then bodies with asymmetries in $I_x$ or $I_y$ up to $x$ parts per million could be reoriented by the same impulses used for the $I_x \equiv I_y$ results. Thus, the $I_x \equiv I_y$ results can be used for small asymmetries to the extent that errors can be accepted in the terminal values for $\theta$ and $\phi$. For larger asymmetries, the other asymmetric curves can be used. Average costs in figure 7 are seen to increase with $I_x/I_y$, $I_z/I_y$, and $R_{2,max}$. In the region $1 - I_z/I_y \to 0$ and for $I_x \to 0$, reorientation costs approach $(\pi/4)R_{2,av}$ as derived in appendix C. The same costs apply also to the region $(1 - I_z/I_y) \to 1$ where $I_z \to 0$. These results are plotted in figure 7.

Although two-impulse coning solutions were not obtained for general reorientations of asymmetric bodies, such solutions can reasonably be anticipated because the three input quantities to the maneuver (coordinate axes torques) should allow control of three output quantities (final Euler angles) regardless of body inertial configuration. Such solutions may result in smaller maneuver costs than the three-impulse asymmetric results of figure 7.

Figure 8 was prepared to illustrate the effect of $R_{2,max}$ on average cost for axisymmetric bodies. Average cost is seen to increase with maneuver range, particularly for small maneuver ranges. A similar plot for asymmetric bodies is shown in figure 9. Although these results are for the set of bodies having $I_x/I_y = 1.2$, they are typical of other $I_x/I_y$ sets.

Thus far, results have been presented for general reorientations. Similar results are available for spin-axis reorientations. The effect of inertial distribution on the cost of spin-axis reorientations is illustrated in figure 10 for maneuver ranges of $\pi$, $\pi/2$, $\pi/4$, and 0.00873 radians. Reorientation costs for axisymmetric bodies ($I_x/I_y \equiv 1$) appear to be relatively insensitive to the inertia configuration. Costs for asymmetric bodies tend to be smaller for elongated bodies. As would be expected, a comparison of figures 7 and 10 shows considerably smaller costs for spin-axis reorientations than for general reorientations.

The cost relationship with maneuver range for spin-axis maneuvers of roll-symmetric bodies is shown in figure 11. By definition, the final roll attitude for spin-axis reorientations is arbitrary. This not only eliminates the need for a follow-up spin maneuver, but greatly increases the number of candidate coning solutions; both of these factors act to reduce maneuver costs significantly and in proportion to the spin inertia $I_z$ as evidenced by a comparison of figures 8 and 11.

Spin-axis maneuver costs for asymmetric bodies of the set $I_x/I_y = 1.2$ are shown in figure 12 as a function of maneuver range for a range of values of $1 - I_z/I_y$. Again, spin-axis maneuver costs are relatively small, increase with maneuver range, and are less sensitive (than general reorientations) to changes in $I_z$ because final attitude about the spin axis is arbitrary.

The average cost results presented in this paper for asymmetric bodies represent minimum cost reorientations involving a mixture of polhodes about the x- and z-axes. Although polhode axes for minimum maneuver cost are unpredictable for individual reorientations, a decided preference for polhodes to surround the axis of smallest inertia is observed. An even stronger tendency is for polhodes to be about z for small $R_2$; however, as $R_2$ becomes larger, the likelihood for polhode about x increases. Similarly, the relative cost of inward compared with outward nutations is not predictable for individual maneuvers. However, it is noticed that inward nutations (opposed mainly by $I_x$) are generally associated with lower coning costs for bodies with $I_x < I_y$ and also that outward nutations (opposed mainly by $I_y$) are usually associated with lower costs for bodies with $I_x > I_y$.

Maneuver costs have been presented in the form of average cost for specified maneuver ranges. A measure of how costs are dispersed about these average

values is given by their standard deviation. Ratios of standard deviation to average cost were computed for all inertial distributions and for maneuver ranges of 0.00873, $\pi/4$, $\pi/2$, and $\pi$ radians. These ratios were found to be moderately constant within each class of inertial distribution and maneuver range. For this reason only the mean value $\bar{r}$ and standard deviation $\sigma$ of these ratios are presented in the following table as a function of maneuver range and type of body symmetry for both general and spin-axis reorientations:

| Maneuver range, $R_{2,max}$, radians | Type of body symmetry | | | |
|---|---|---|---|---|
| | Axisymmetric, $I_x = I_y \neq I_z$ | | Asymmetric, $I_x \gtrless I_y \gtrless I_z$ | |
| | Mean value of ratio, $\bar{r}$ | Standard deviation of ratio, $\sigma$ | Mean value of ratio, $\bar{r}$ | Standard deviation of ratio, $\sigma$ |
| General reorientations | | | | |
| 0.00873 | 0.572 | 0.004 | 0.430 | 0.024 |
| $\pi/4$ | .438 | .074 | .341 | .020 |
| $\pi/2$ | .379 | .041 | .320 | .016 |
| $\pi$ | .341 | .041 | .320 | .032 |
| Spin-axis reorientations | | | | |
| 0.00873 | 0.358 | 0.002 | 0.575 | 0.023 |
| $\pi/4$ | .368 | .006 | .433 | .058 |
| $\pi/2$ | .385 | .006 | .367 | .030 |
| $\pi$ | .417 | .008 | .366 | .041 |

## CONCLUDING REMARKS

This report presents data figures which can be used to determine average costs of reorientation by impulse coning for bodies of all possible inertial distribution and over a wide range of maneuver angles for spin-axis reorientations as well as general reorientations. Impulse coning is a method of attitude reorientation in which impulsive torques are used to initiate and later to terminate free precessional motion of a body. In spin-axis reorientations, the final rotational attitude about the spin axis is not specified.

All attitude reorientations of axisymmetric bodies can be accomplished with two-impulse coning. Moreover, for any given reorientation, minimal two-impulse coning costs are always less than three-impulse (coning plus spin maneuver) reorientation costs.

All general reorientations of asymmetric bodies achieved by the impulse coning method and constrained to have equal initial and final angles between the spin axis and the angular momentum vector are found to require a spin correction maneuver at the end of coning. As a result, average costs of reorientation are considerably larger than those for axisymmetric bodies. However,

it is believed that the aforementioned constraint can be eliminated from coning reorientations of asymmetric bodies with the result that spin correction maneuvers would not be needed and average costs of reorientation could be reduced.

Spin-axis attitude reorientations of bodies of any inertial distribution can be accomplished with two-impulse coning maneuvers. Average costs of spin-axis reorientations are considerably less than similar costs for general reorientations, especially for foreshortened bodies.

Langley Research Center
National Aeronautics and Space Administration
Hampton, VA 23665
June 15, 1977

# APPENDIX A

## PROGRAM ASYMCON

The computer program ASYMCON, used to determine minimum costs for attitude reorientation of asymmetric bodies by the impulse coning method, is presented in this appendix.

### Symbols

Pertinent symbols used in program ASYMCON and their definition or relationship to symbols used throughout the report are as follows:

| | |
|---|---|
| A | indicates polhode about x-axis |
| ACOST | weighted average cost of maneuvers within given $R_{2,max}$, $\frac{\Sigma(Q_{3,min}\lvert\sin R_2\rvert)}{\Sigma(\lvert\sin R_2\rvert)}$ |
| C | indicates polhode about z-axis |
| DEL | $\theta_o$ |
| FLAG | FLAG |
| IX,IY,IZ | $I_x$, $I_y$, and $I_z$, respectively |
| PI | $\pi$ |
| QR | $t_s/t_f$ |
| RF | $0.5\left(1 + \frac{\lvert\psi_f\epsilon\rvert}{\psi_f\epsilon}\right)Q_{2,A}$ |
| R1,R2,R3 | $R_1$, $R_2$, and $R_3$, respectively |
| R1C,R2C,R3C | maneuver about x polhode axis equivalent to $R_1,R_2,R_3$ maneuver about z polhode axis |
| $R_{12}$ | $\theta_o$ |
| R12A | $\theta_{av}$ |
| R12M | extremum value of $\theta$ |
| R18 | F |
| R20 | $\Delta\phi$ |

| | |
|---|---|
| R201 | latest value of $\Delta\phi$ |
| R21 | $\phi_o$ |
| R26 | $Q_{3,min}$ |
| R29 | $\epsilon$ |
| R31 | $Q_2$ |
| R32 | $2\|\epsilon\|I_z/I_y$ |
| R4,R5,R6 | $I_x$, $I_y$, and $I_z$, respectively |
| R40,R41 | lower and upper sample limit for $R_1$, respectively |
| R42,R43 | lower and upper sample limit for $R_2$, respectively; R43 = $R_{2,max}$ |
| R44,R45 | lower and upper sample limit for $R_3$, respectively |
| R54 | absolute value of $\sin R_2$; used as weighting factor for calculating average cost |
| R7 | $\psi_f$ |
| R9 | $\psi_s$ |
| SD | standard deviation of average cost |
| SGN7 | $0.5\left(1 - \frac{\psi_f}{\|\psi_f\|}\right)$ |
| SR4 | temporary storage for $I_x$ or $I_z$ during polhode change |
| TCOST | weighted sum of maneuver costs |
| TC2 | weighted sum of squared maneuver costs |
| TNO | weighted sum of maneuvers |

# APPENDIX A

## Program Listing

```
      PROGRAM ASYMCON (INPUT,OUTPUT,TAPE5=INPUT,TAPE6=OUTPUT)
      COMMON R1,R2,R4,R5,R6,R7,R9,R12,R18,R20,PI,FLAG,R12A,SGN7,R21,R201
      COMMON CHANGE,R35,R37
      REAL IX,IY,IZ
      REAL M11,MO11,MF11,M12,MO12,MF12,M13,MO13,MF13
      REAL M21,MO21,MF21,M22,MO22,MF22,M23,      MF23
      REAL M31,MO31,MF31,M32,MO32,MF32,M33,MO33,MF33
      INTEGER CSAV
      INTEGER A,C,A1,CA1
      EQUIVALENCE(IX,R4),(IY,R5),(IZ,R6)
      DATA A,C/1HA,1HC/
      NAMELIST/ICONE/IX,IY,IZ,CON,PTDEN,R40,R41,R42,R43,R44,R45,PRINT,SR
      PI=2.*ASIN(1.)$R8=180./PI$CON=1. $ PRINT=1. $ IY=100. $ SR=0.
      PTDEN=8./PI $ CON=2. $ R40=R42=0. $ R44=-PI $ R41=R43=R45=PI
      PTDEN=16./PI $ R43=PI/2.
 1000 READ(5,ICONE)
      IF(EOF(5))14,15
   14 STOP
   15 CONTINUE
      R70=REP=0. $ C26=1.E8 $ TNO=TCOST=TC2=0. $ ISAV=0 $ FLAG=0.
      KOUNT=0 $ START=-1.E-6 $ TCREP=0.
      R1=PR1=R51=R40+1./(2.*PTDEN)
      R2=PR2=R42+1./(2.*PTDEN)
      R3=PR3=R53=R44+CON/(2.*PTDEN)
      WRITE(6,ICONE)
      R54=ABS(SIN(R2)) $ GO TO 2
    7 R3=PR3=R3+CON/PTDEN $ IF(R3.GT.R45)GO TO 25 $ GO TO 2
    8 R1=PR1=R1+1./PTDEN $ IF(R1.GT.R41)GO TO 24 $ GO TO 2
    9 R2=PR2=R2+1./PTDEN $ R54=ABS(SIN(R2)) $ IF(R2.GT.R43)GO TO 26
C   COMPUTE EULER COSINE MATRIX FOR MANEUVER R1,R2,R3 ABOUT Z Y Z AXES
    2 SR1=SIN(R1) $ SR2=SIN(R2) $ SR3=SIN(R3)
      CR1=COS(R1) $ CR2=COS(R2) $ CR3=COS(R3)
      B11=CR1*CR2*CR3-SR1*SR3 $ B12=SR1*CR2*CR3+CR1*SR3
      B13=-SR2*CR3 $ B21=-CR1*CR2*SR3-SR1*CR3
      B22=-SR1*CR2*SR3+CR1*CR3 $ B23=SR2*SR3
      B31=SR2*CR1 $ B32=SR2*SR1 $ B33=CR2
C   COMPUTE EULER ROTATIONS R1C, R2C,R3C ABOUT -X Y -X AXES
      R1C=ATAN2(B12,-B13) $ X3=-B33*SIN(R1C)-B32*COS(R1C)
      Y3=B22*COS(R1C)+B23*SIN(R1C) $ X2=B21*X3+B31*Y3 $ Y2=B11
      R2C=ATAN2(X2,Y2) $ R3C=ATAN2(X3,Y3)
    3 IF(REP.EQ.0.)GO TO 1 $ R1=-R1C $ R2=R2C $ R3=-R3C
C   INITIALIZE FOR NEWTON RAPHSON ITERATION METHOD
    1 CHANGE=0. $ SGN7=0. $ IF(ISAV.GT.1.)SGN7=1. $ KOUNT=0
      Q=(R4-R6)*(.5-SGN7) $ R20=S61=-ABS(Q)/Q*START
```

```
      CALL ASYITER $ IF(CHANGE.EQ.1.)GO TO 18
      S71=R201
      R20=S62=(R20+R201)/2.
      CALL ASYITER $ IF(CHANGE.EQ.1.)GO TO 18
      S72=R201
  101 R100=(S72-S71)/(S62-S61)
      R20=S63=(S71-R100*S61)/(1.-R100)
      KOUNT=KOUNT+1 $ IF(KOUNT.EQ.11)GO TO 18
      CALL ASYITER $ IF(CHANGE.EQ.1.)GO TO 18
      S73=R201
C  ACCEPTANCE CONDITION FOR ITERATION
      IF(.001/R8.GT.ABS((R20-R201)/R20))GO TO 31
      S61=S62 $ S62=S63 $ S71=S72 $ S72=S73
      GO TO 101
   31 R21=-R1+PI/2.+R9/2.+PI*SGN7
C  COMPUTE COSTS OF MANEUVER
      R22=ABS(2.*SIN(R12)*R7*R4/R18)/R5
      R23=ABS(2.*COS(R12)*R7*R4/R18)/R5
      R29=R1+R3-R9-R20 $ R29=R29-2.*PI*INT(R29/(2.*PI))
      R31=R22*(ABS(SIN(R21))+ABS(COS(R21))+ABS(SIN(R20+R21))+ABS
     1(COS(R20+R21)))/2.+R23
C   MINIMIZING COST OF SPIN CORRECTION MANEUVER
      R32=2.*R6/R5*ABS(R29)
      RF=R23*.5*(1.+ABS(R7/R29)/(R7/R29)) $ QR=SQRT(R32/(R31-RF))
      IF(QR.GT.R32/R23)QR=R32/R23 $ R26=(R31-RF)*(1.+QR)+R32+R32/QR
      A29=R29-2.*PI*ABS(R29)/R29 $ R32=2.*R6/R5*ABS(A29)
      RF=R23*.5*(1.+ABS(R7/A29)/(R7/A29)) $ AQR=SQRT(R32/(R31-RF))
      IF(AQR.GT.R32/R23)AQR=R32/R23 $ A26=(R31-RF)*(1.+AQR)+R32+R32/AQR
      IF(A26.GE.R26)GO TO 60 $ QR=AQR $ R26=A26 $ R29=A29
   60 R26=R26*(1.-SR)+R31*SR
C  POLHODE CONDITION DETERMINED
      A1=A $ IF((REP-.5)*R35/R37.LT.0.)A1=C
C  LOWEST COST SOLUTION IS SAVED
      IF(R26.GE.C26)GO TO 18
      C7=R7 $ C9=R9 $ C20=R20 $ DEL=R12 $ C12A=R12A $ CA1=A1
      C26=R26 $ C29=R29 $ C31=R31  $ C21=R21  $ CSAV=ISAV
      CREP=REP $ CCR1=R1 $ CCR2=R2 $ CCR3=R3 $ CQR=QR
      CSTART=-ABS(Q)/Q*START
   18 ISAV=ISAV+1 $ FLAG=0. $ IF(ISAV.EQ.1)FLAG=1.
      IF(ISAV.EQ.3)FLAG=1. $ IF(ISAV.LT.4)GO TO 1 $ ISAV=0
C  SETTING CONDITIONS FOR POLHODE ABOUT(A) AXIS OR RESETTING FOR
C  POLHODE ABOUT (C) AXIS
    6 SR4=R4 $ R4=R6 $ R6=SR4
      IF(REP.GT.0.)GO TO 5 $ REP=REP+1. $ GO TO 3
```

```
    5 REP=0. $ R1=PR1 $ R2=PR2 $ R3=PR3
C   RESETTING INITIAL VALUE OF R20 FOR ITERATION
      IF(ABS(START).NE.1.E-6)GO TO 11 $ START=-.5 $ GO TO 3
   11 IF(C26.LT.1.E8)GO TO 13 $ START=-2.*START
      IF(ABS(START).LT.5.)GO TO 3 $ CSTART=-ABS(Q)/Q*START $ GO TO 16
C   COMPUTE STATISTICALLY AVERAGE MANEUVER COST
   13 TNO=TNO+R54 $ TCOST=TCOST+C26*R54 $ ACOST=TCOST/TNO
      TC2=TC2+C26*R54*C26
      TCREP=TCREP+CREP
      R70=R70+1. $ IF(PRINT.EQ.0.)GO TO 27
C   MATRIX TRANSFORMATION CHECK FOR EACH MANEUVER
   10 S20=S2F=SIN(DEL) $ C20=C2F=COS(DEL) $ S30=SIN(C21)
      C30=COS(C21) $ S1F=SIN(C7) $ C1F=COS(C7) $ S3F=SIN(C20+C21)
      C3F=COS(C20+C21) $ S1=SIN(CCR1) $ C1=COS(CCR1) $ S2=SIN(CCR2)
      C2=COS(CCR2) $ S3=SIN(CCR3-C29) $ C3=COS(CCR3-C29)
      MO11=C20*C30                    $ MO31=-S20*C30
      M11=-S1*S3+C1*C2*C3             $ M31=-S2*C3
      MF11=-S1F*S3F+C1F*C2F*C3F       $ MF31=-S2F*C3F
      MO12=-C20*S30                   $ MO32=S20*S30
      M12=-S1*C3-C1*C2*S3             $ M32=S2*S3
      MF12=-S1F*C3F-C1F*C2F*S3F       $ MF32=S2F*S3F
      MO13=S20                        $ MO33=C20
      M13=C1*S2                       $ M33=C2
      MF13=C1F*S2F                    $ MF33=C2F
      MO21=S30
      M21=C1*S3+S1*C2*C3,
      MF21=C1F*S3F+S1F*C2F*C3F
      MO22=C30
      M22=C1*C3-S1*C2*S3
      MF22=C1F*C3F-S1F*C2F*S3F
      M23=S1*S2
      MF23=S1F*S2F
      D11=MO11*M11+MO12*M21+MO13*M31-MF11
      D12=MO11*M12+MO12*M22+MO13*M32-MF12
      D13=MO11*M13+MO12*M23+MO13*M33-MF13
      D21=MO21*M11+MO22*M21-MF21
      D22=MO21*M12+MO22*M22-MF22
      D23=MO21*M13+MO22*M23-MF23
      D31=MO31*M11+MO32*M21+MO33*M31-MF31
      D32=MO31*M12+MO32*M22+MO33*M32-MF32
      D33=MO31*M13+MO32*M23+MO33*M33-MF33
      IF(ABS(D11)+ABS(D12)+ABS(D13)+ABS(D21)+ABS(D22)+ABS(D23)+ABS(D31)
     1+ABS(D32)+ABS(D33).GT..0001)
     1WRITE(6,53)D11,D12,D13,D21,D22,D23,D31,D32,D33
```

```
   53 FORMAT(1X9E11.3/)
   16 CONTINUE
      WRITE(6,28)CCR1,CCR2,CCR3,C7,CREP,CSAV,CSTART,C21,DEL,C26,C12A,
     1C9,C20,ACOST,R70,C29,CA1,PR1,PR2,PR3,CQR
   28 FORMAT(1XF8.4,F7.4,2F8.4,F3.0,I1,F4.1,F8.4,F7.4,F7.3,F7.4,2F8.4,
     1F5.2,F6.0,F8.4,1XA1,F6.2,F5.2,F6.2,F5.2,F3.0)
   27 C26=1.E8 $ START=-1.E-6 $ GO TO 7
   25 R3=PR3=R53 $ GO TO 8
   24 R1=PR1=R51 $ SD=SQRT(TC2/TNO-ACOST*ACOST) $ SDA=SD/ACOST
      WRITE(6,4)R2,TNO,TCREP,ACOST,SD,SDA
      GO TO 9
    4 FORMAT(6X8E14.4)
   26 SD=SQRT(TC2/TNO-ACOST*ACOST) $ SDA=ACOST/SD
      WRITE(6,4)R70,TNO,TCREP,ACOST,SD,SDA
      GO TO 1000
      END
      SUBROUTINE ASYITER
C  THIS SUBROUTINE ITERATIVELY COMPUTES A SOLUTION SET OF VALUES FOR THE
C  VARIABLES INFLUENCING THE NUTATIONAL MOTION OF THT MANEUVERING BODY
      COMMON R1,R2,R4,R5,R6,R7,R9,R12,R18,R20,PI,FLAG,R12A,SGN7,R21,R201
      COMMON CHANGE,R35,R37
      R18=(R4+R5)/(2.*R5)+(1.-2.*FLAG)*(R5-R4)/(2.*R5)*SIN(R20)/R20
      R21=-R20/2.+PI/2.*FLAG
      R9=2.*(R21+R1-PI/2.-PI*SGN7) $ R9=R9-2.*PI*INT(R9/(2.*PI))
      R12=ABS(ATAN(TAN(R2/2.)/SIN(R9/2.)))
      F1=TAN(R21) $ F2=COS(R21) $ F3=TAN(R12)
      R35=R5*(R6-R4)+R4*(R6-R5)*F1*F1
      R36=R6*(R5-R4)*F1*F1+R5*(R6-R4)/(F3*F3*F2*F2)
      R37=R6*(R4-R5)+R4*(R6-R5)/(F3*F3*F2*F2)
      IF(R35/R37.GT.0.)GO TO 5 $ CHANGE=1. $ RETURN
    5 R12M=ATAN(SQRT(R35/R36)) $ IF(FLAG.EQ.1.)R12M=ATAN(SQRT(R35/R37))
      R12A=(R12+R12M)/2. $ DIFF=R12M-R12 $ DIFS=SIN(R12M)-SIN(R12)
      IF(ABS(DIFF).GT..001)R12A=ACOS(DIFS/DIFF)
      R7=2.*ASIN(COS(R2/2.)*SIN(R9/2.)/COS(R12))
C   R7 PLACED INTO PROPER QUADRANT
      R50=ABS(R9)/R9 $ R51=INT(R9/PI)+R50 $ R51=INT(R51/2.)
      IF(R51/2..EQ.INT(R51/2.))GO TO 1 $ R7=2.*R51*PI-R7 $ GO TO 2
    1 R7=2.*R51*PI+R7
C  COMPUTE LATEST VALUE FOR R20
    2 R201=R7*COS(R12A)*(R4/R18-R6)/R6
      RETURN $ END
```

## APPENDIX B

## INERTIA CONSTRAINTS

The following derivation generates boundaries for identification of all possible inertial distributions.

The class of all rigid bodies is divided into two parts. Consider for the first part those bodies having

$$I_x \geqq I_y \geqq I_z \tag{B1}$$

where $I_y$ is intermediate inertia and $I_z$ is spin inertia. From the definitions

$$I_x = \Sigma\left[m(y^2 + z^2)\right]$$

$$I_y = \Sigma\left[m(x^2 + z^2)\right]$$

$$I_z = \Sigma\left[m(x^2 + y^2)\right]$$

it is apparent that inertia about any one of the three axes cannot exceed the sum of inertias about the other two axes. Thus, it follows that

$$I_x \leqq I_y + I_z \tag{B2}$$

From condition (B1), the following relationships can be obtained:

$$1 - \frac{I_z}{I_y} \geqq 0 \qquad \frac{I_x}{I_y} \geqq 1 \tag{B3}$$

From condition (B2)

$$I_x - I_z \leqq I_y \tag{B4}$$

Adding $I_y$ to both sides of inequality (B4) and dividing by $I_y$ give

$$\frac{I_x}{I_y} + \left(1 - \frac{I_z}{I_y}\right) \leqq 2 \tag{B5}$$

Equations (B3) and (B5) define triangular zone A of figure 6 where $I_x \geqq I_y \geqq I_z$.

For the second part, consider all remaining rigid bodies. These are restricted to those bodies having

$$I_x \leqq I_y \leqq I_z \tag{B6}$$

Applying the reasoning just preceding inequality (B2) to the second part yields

$$I_x + I_y \geqq I_z \tag{B7}$$

From condition (B6), the following relationships can be obtained:

$$1 - \frac{I_z}{I_y} \leqq 0 \qquad \frac{I_x}{I_y} \leqq 1 \tag{B8}$$

Dividing inequality (B7) by $I_y$ and rearranging give

$$\frac{I_x}{I_y} + \left(1 - \frac{I_z}{I_y}\right) \geqq 0 \tag{B9}$$

Inequalities (B8) and (B9) define triangular zone B in figure 6 for which $I_x \leqq I_y \leqq I_z$.

Zones A and B include all possible inertial distributions providing $I_y$ is the intermediate moment of inertia.

## APPENDIX C

## AVERAGE REORIENTATION COSTS FOR ROD-SHAPED BODIES

The derivation of the average reorientation costs for rod-shaped bodies is presented in this appendix.

Consider first the configuration $I_x \to 0$ and $1 - I_z/I_y \to 0$, a rod-shaped body along the x-axis. Because $I_x \to 0$, $x$ is the polhode axis and the rod precesses about a momentum vector located in the $y$-$z$ plane with a half-cone angle of $\theta \approx \pi/2$. The average cost of reorientation can be written

$$\text{Average cost} = K \frac{2(\text{Impulse} \times \text{Time})_{\text{mean}}}{I} = \frac{2}{I} K(\text{Momentum} \times \text{Time})_{\text{mean}}$$

$$= \frac{2}{I} K(I\omega t)_{\text{mean}} = 2K\, R_{2,\text{mean}}$$

where $K$ is a factor to account for reaction thrusters fixed relative to the body principal axes and $\omega$ is the amplitude of the angular velocity vector.

Assuming that the direction of the maneuver relative to the transverse thrusters is uniformly distributed about the z-axis,

$$K = \left(|\sin \phi_o| + |\cos \phi_o|\right)_{\text{mean}} = \frac{2}{\pi} \int_0^{\pi/2} (\sin \phi_o + \cos \phi_o) d\phi_o = \frac{4}{\pi}$$

Values of $R_{2,\text{mean}}$ and average cost are listed as follows for selected values of $R_{2,\text{max}}$ used in the body of the paper:

| | | | | |
|---|---|---|---|---|
| $R_{2,\text{max}}$ | $\pi$ | $\pi/2$ | $\pi/4$ | 0.00873 |
| $R_{2,\text{mean}}$ | $\pi/2$ | $\pi/3$ | 0.5480 | 0.00617 |
| Average cost | 4 | 8/3 | 1.461 | 0.0164 |

Finally, for the configuration $1 - I_z/I_y \to 1$ and $I_x \equiv I_y$, the body is a rod along the z-axis. Although the inertial notations have changed relative to the previous configuration, the physical situation is identical as are the reorientation costs.

## REFERENCES


1. Cole, Roy Dale; Ekstrand, Mary Elizabeth; and O'Neill, Michael R.: Attitude Control of Rotating Satellites. ARS J., vol. 31, no. 10, Oct. 1961, pp. 1446-1447.

2. Grubin, Carl: Generalized Two-Impulse Scheme for Reorienting a Spin Stabilized Vehicle. Guidance and Control, Robert E. Roberson and James S. Farrior, eds., Academic Press, 1962, pp. 649-668.

3. Grubin, Carl: Two-Impulse Attitude Reorientation of an Asymmetric Spinning Vehicle. AIAA Symposium on Structural Dynamics and Aeroelasticity, Aug.-Sept. 1965, pp. 245-249.

4. Dixon, M. V.; Edelbaum, T. N.; Potter, J. E.; Vandervelde, W. F.: Fuel Optimal Reorientation of Axisymmetric Spacecraft. Rep. No. SAMSO-TR-70-184, U.S. Air Force, Mar. 15, 1970. (Available from DDC as AD 706 386.)

5. Greenwood, Donald T.: Principles of Dynamics. Prentice-Hall, Inc., c.1965, pp. 398-399.

6. Thomson, William Tyrrell: Introduction to Space Dynamics. John Wiley & Sons, Inc., c.1961, pp. 125-126.

7. Meyer, George; Lee, Homer Q.; and Wehrend, William R., Jr.: A Method for Expanding a Direction Cosine Matrix Into an Euler Sequence of Rotations. NASA TM X-1384, 1967.

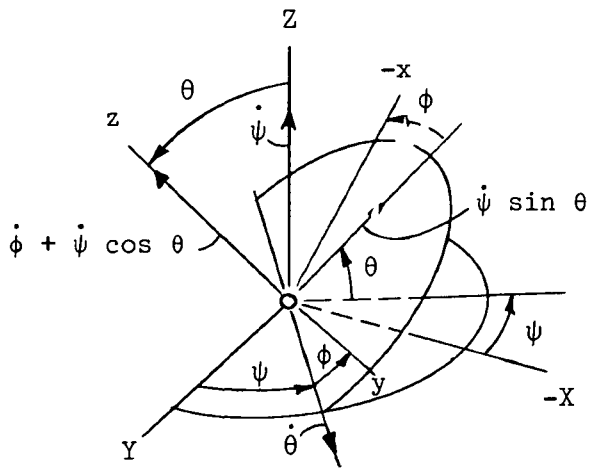


(a) Inertial rate components.

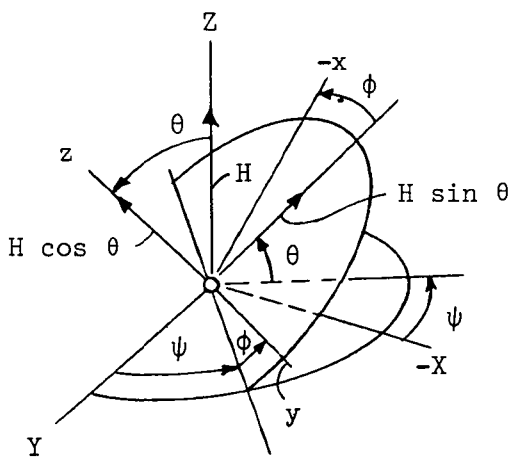


(b) Angular momentum components.

Figure 1.- Orientation of body and inertial coordinate axis systems for Euler rotation sequence $\psi,\theta,\phi$ about body axes z,y,z, respectively.

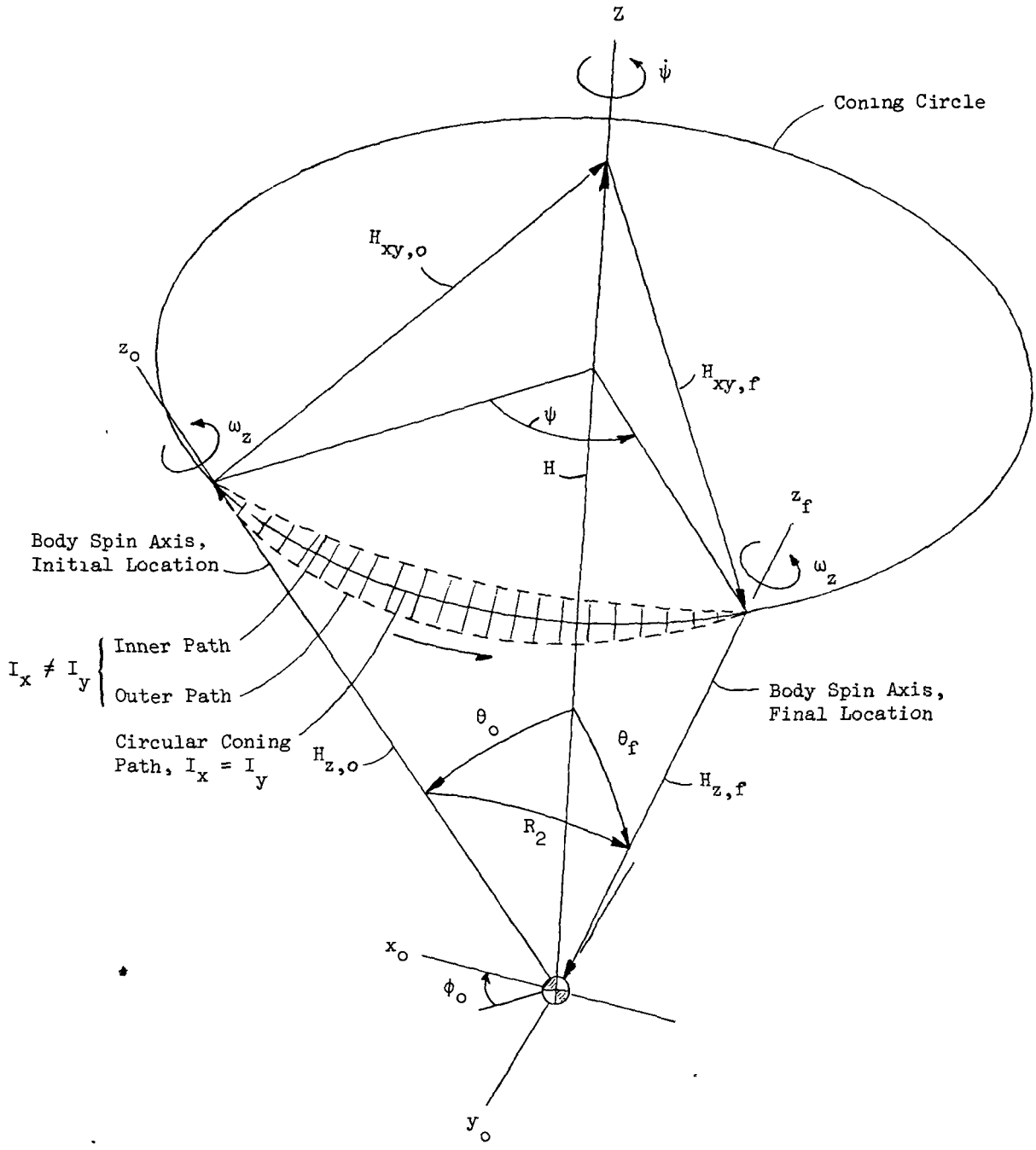


Figure 2.- Coning geometry showing momentum components.

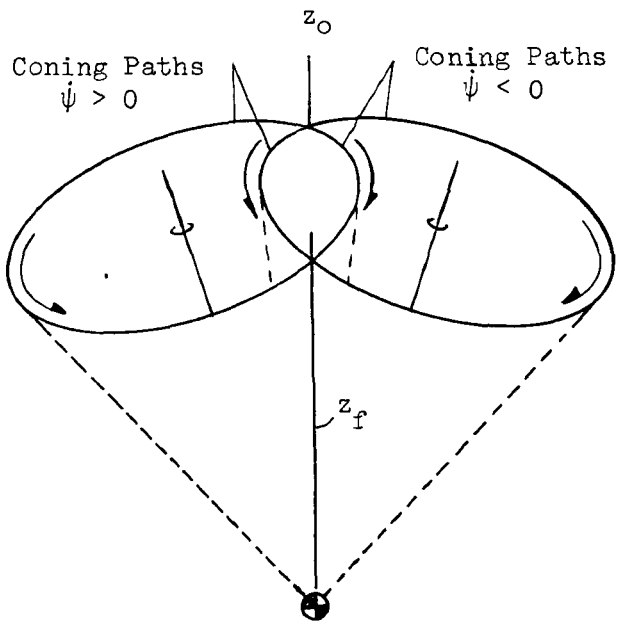


Figure 3.- Symmetric solution pairs showing cone geometry and alternative paths for positive and negative coning rates.

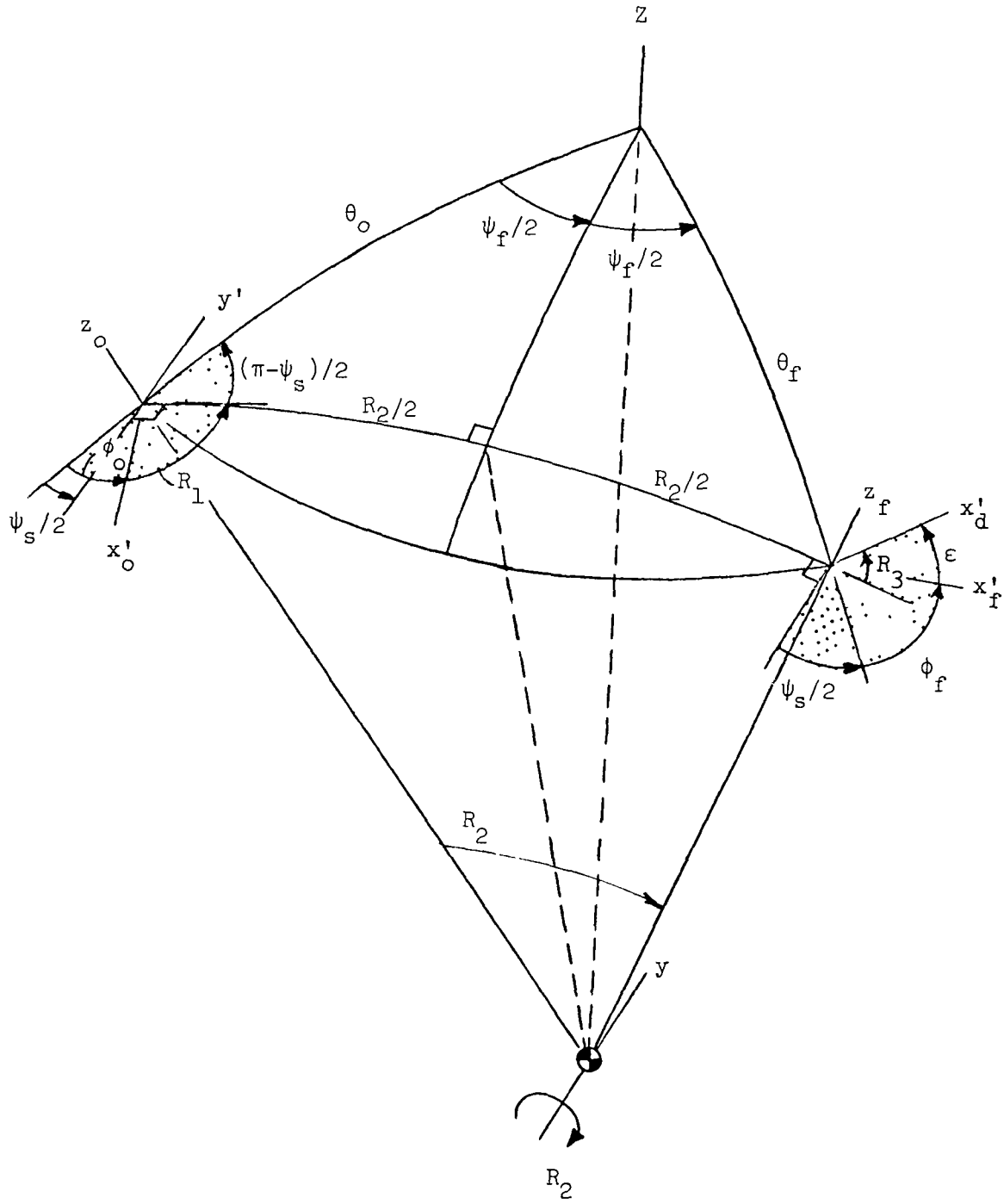


(a) Positive precession rates.

Figure 4.- Spherical geometry of generalized maneuver $R_1, R_2, R_3$, illustrating spin-angle relationships. Positive angles measured clockwise about axis of rotation.

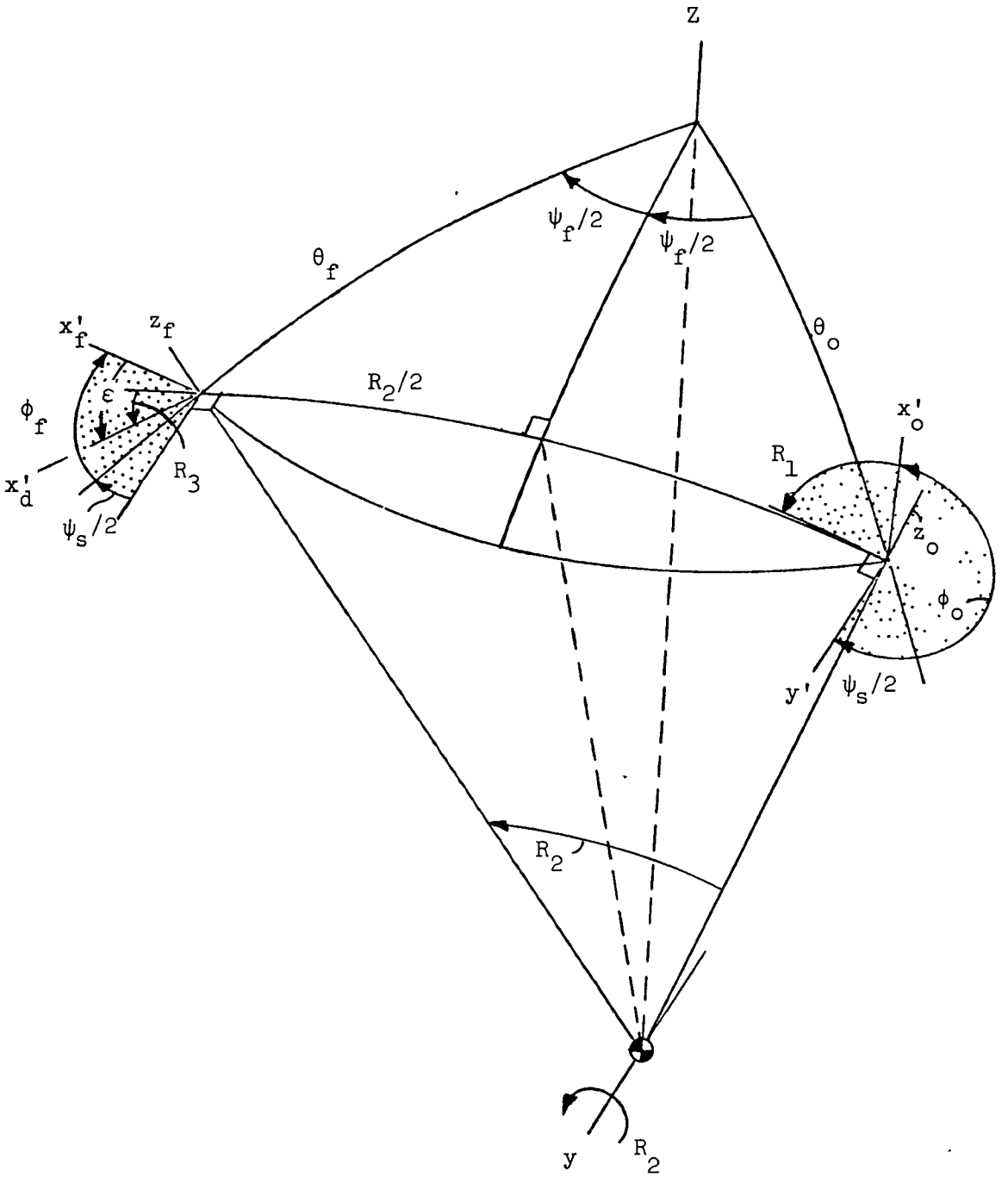


(b) Negative precession rates.

Figure 4.- Concluded.

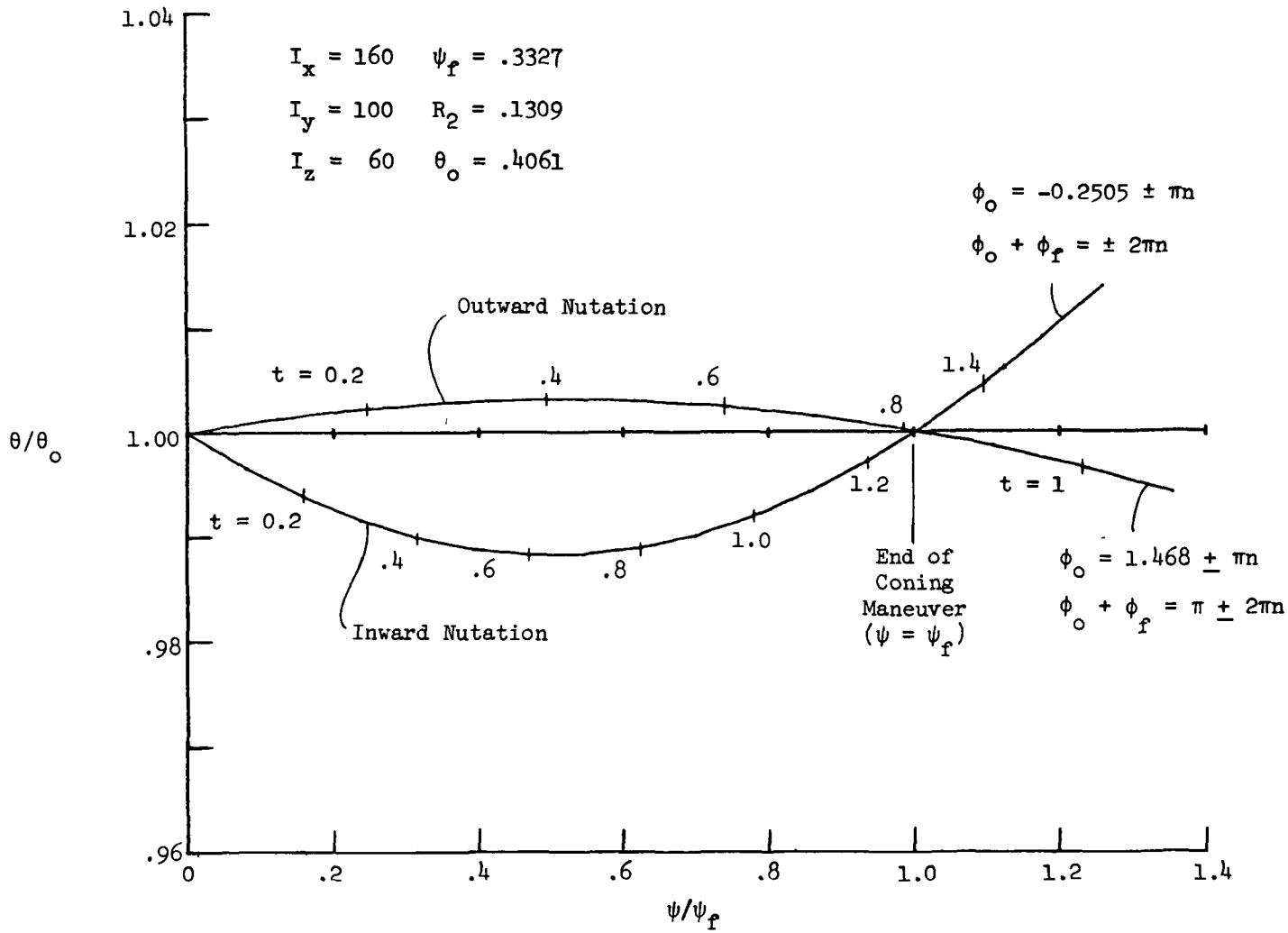


Figure 5.- Integrated solution trajectories for example maneuver, showing inward and outward nutation classes.

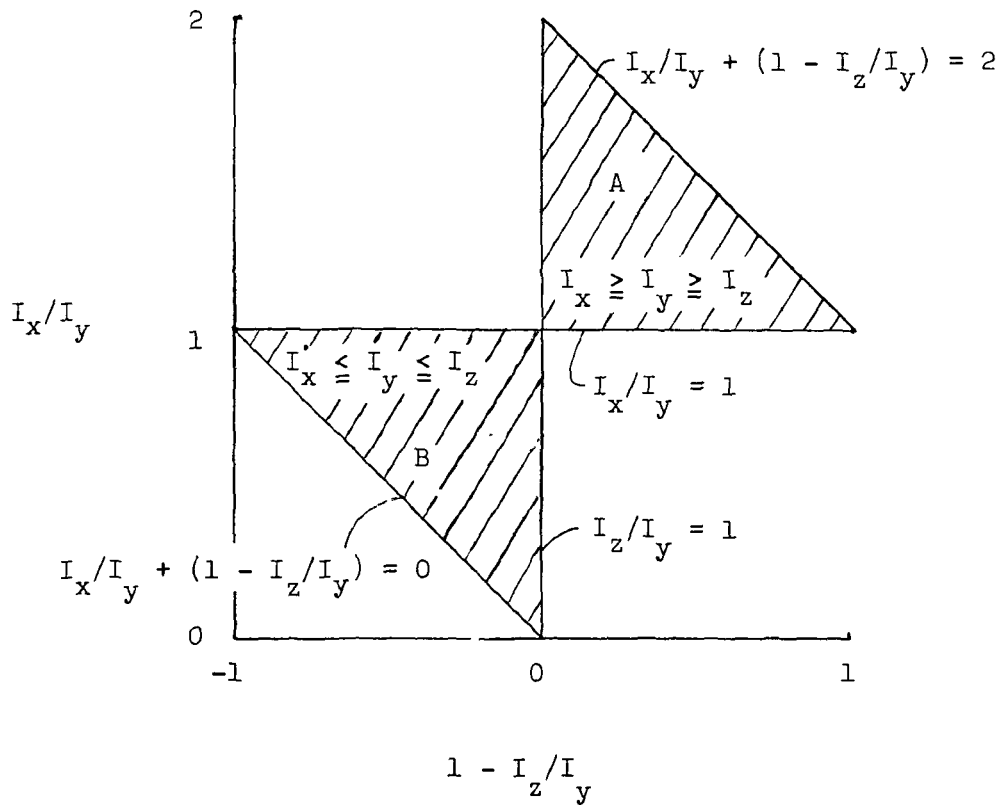


Figure 6.- Inertia constraints.

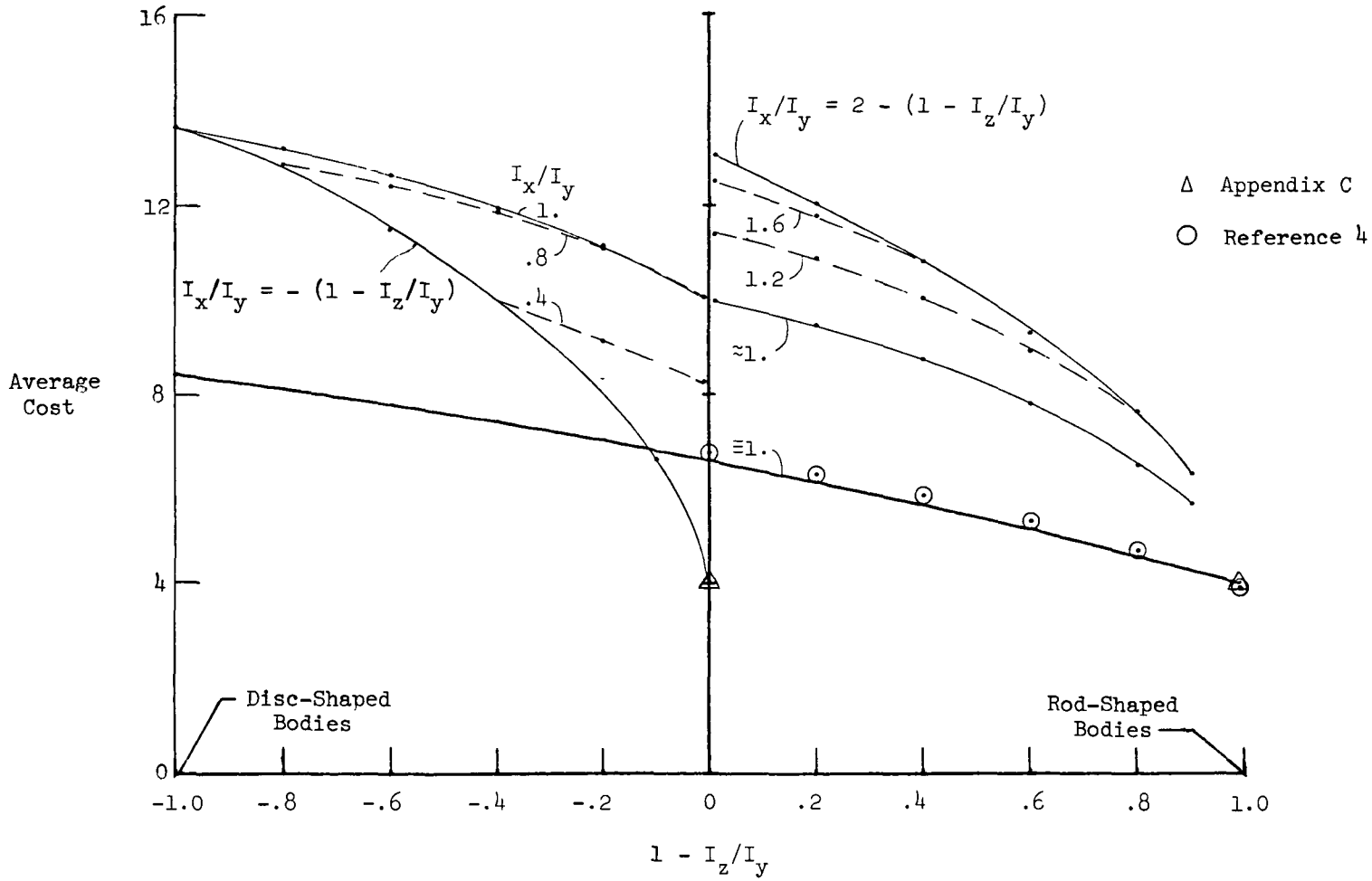


(a) Maneuver range = π radians. (All possible reorientations.)

Figure 7.- Effect of inertia distribution on average cost of reorientation.

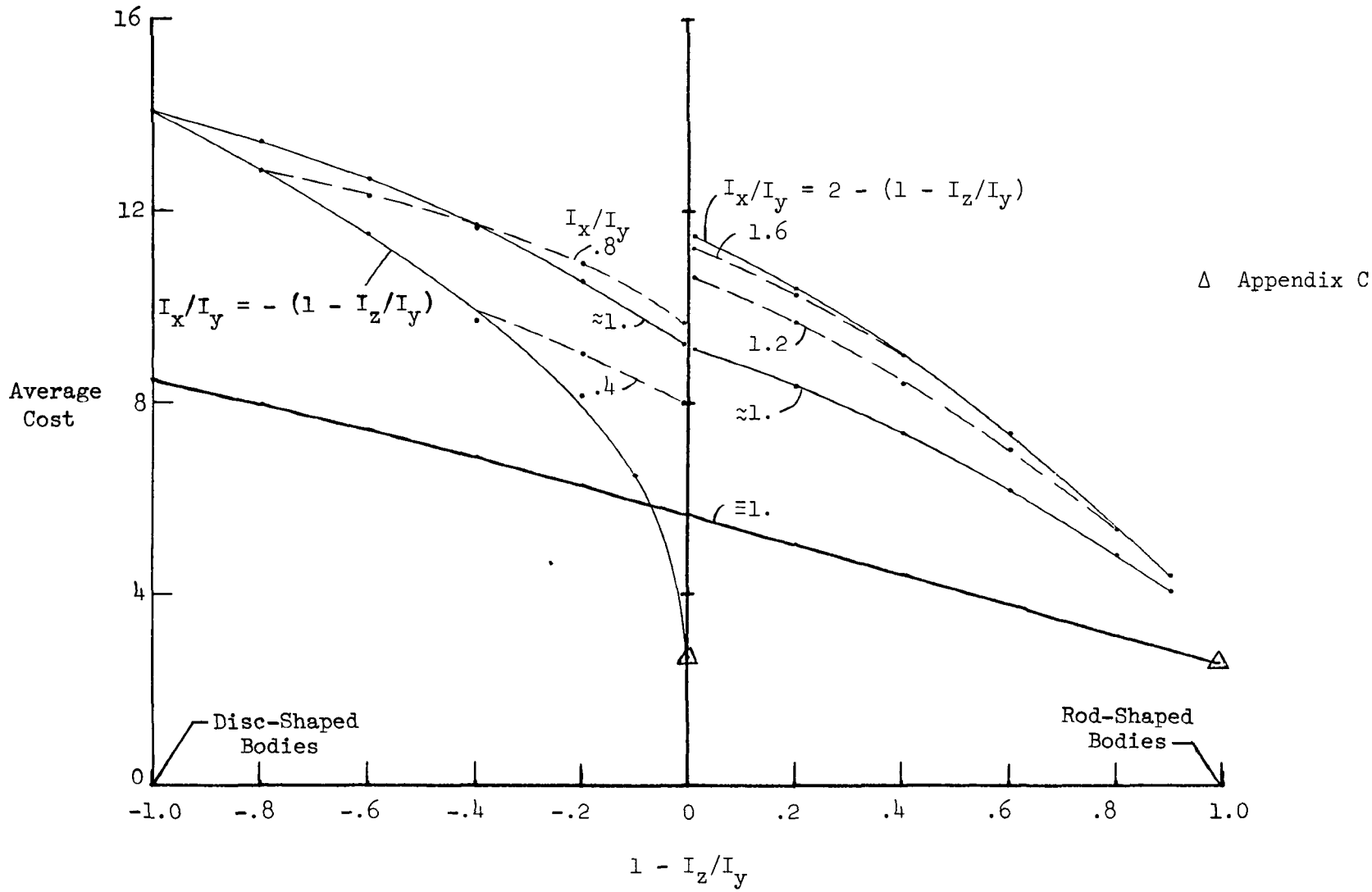


(b) Maneuver range = π/2 radians.

Figure 7.- Continued.

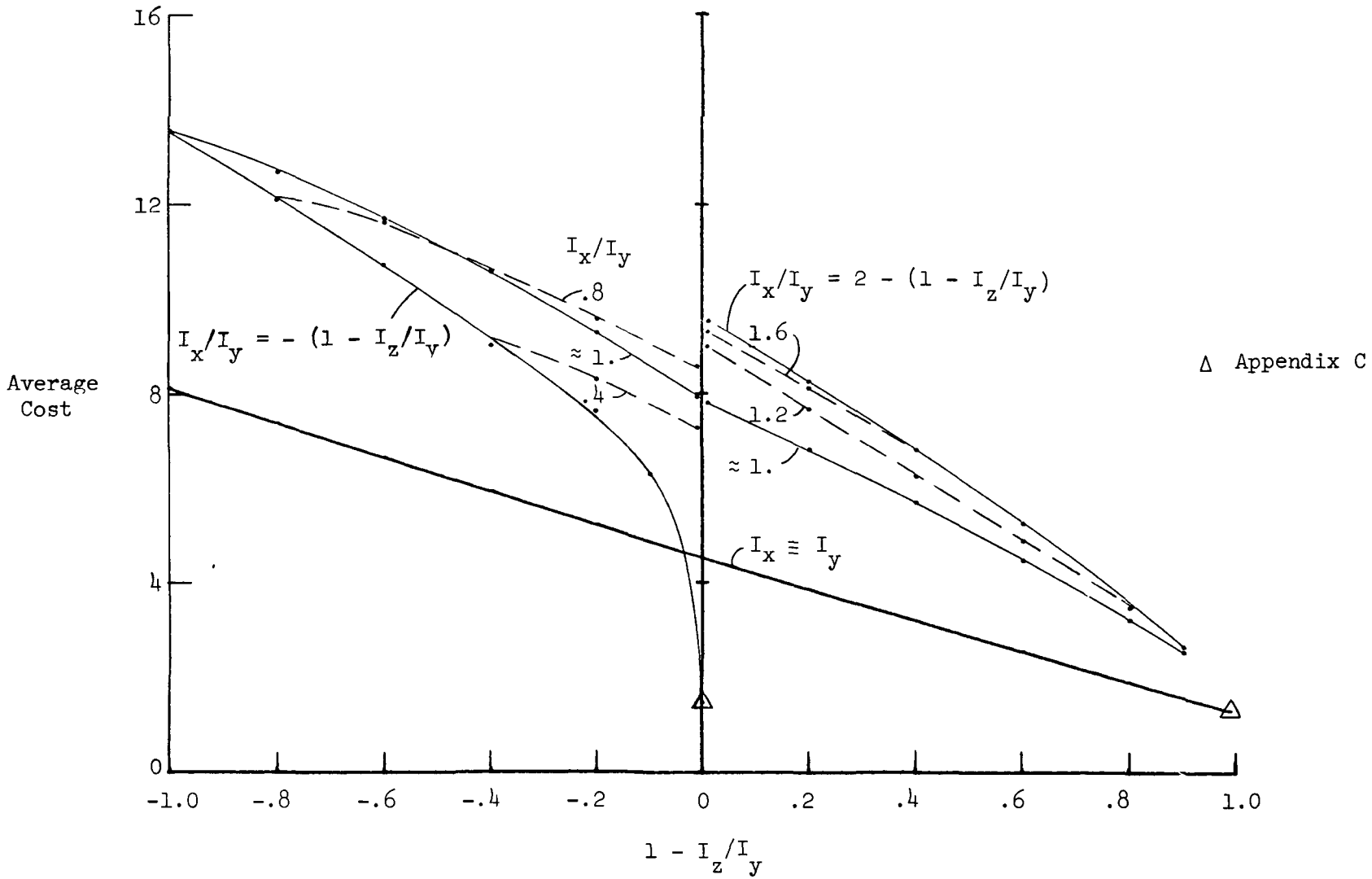


(c) Maneuver range = π/4 radians.

Figure 7.- Continued.

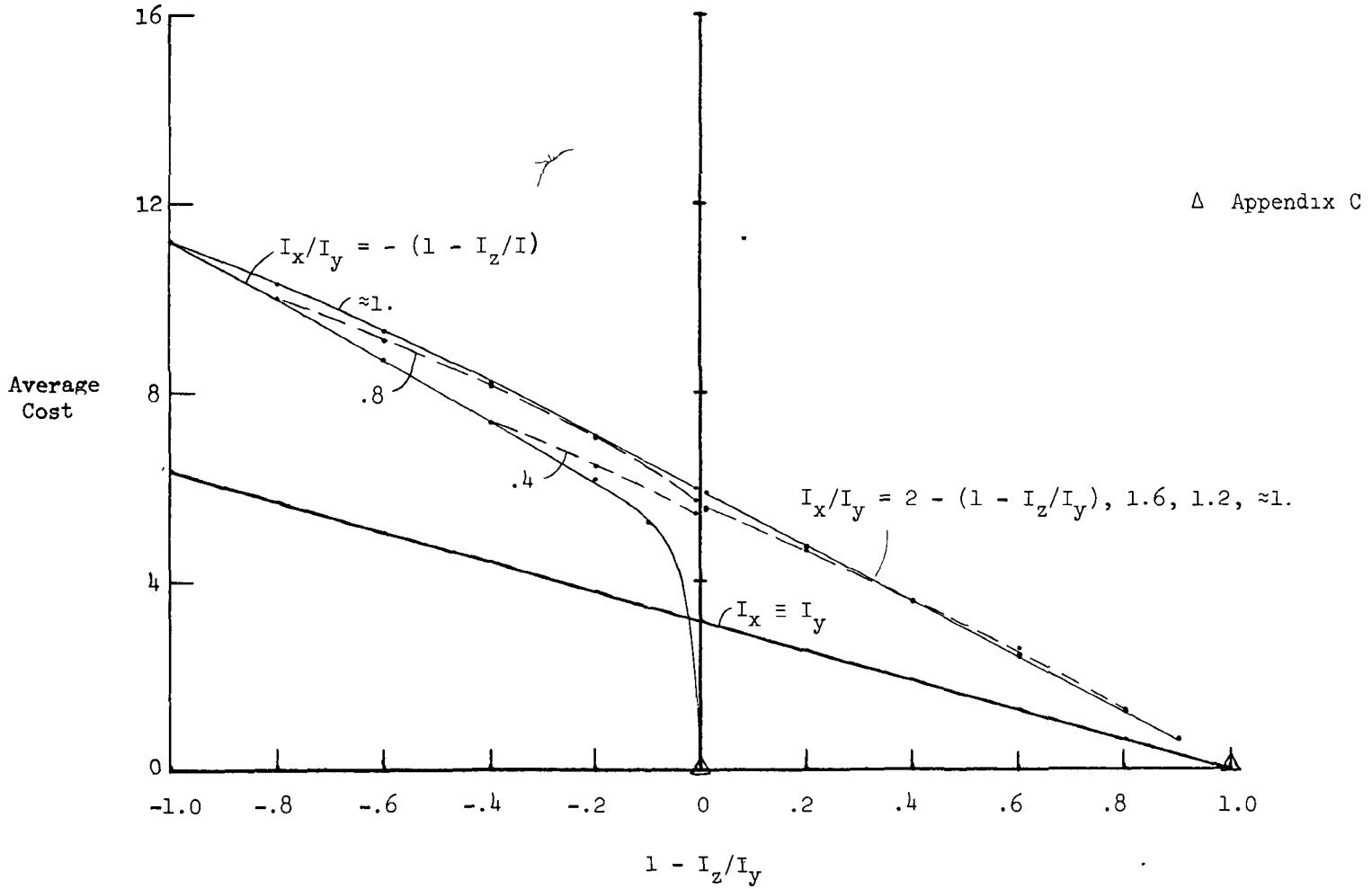


(d) Maneuver range = 0.00873 radian.

Figure 7.- Concluded.

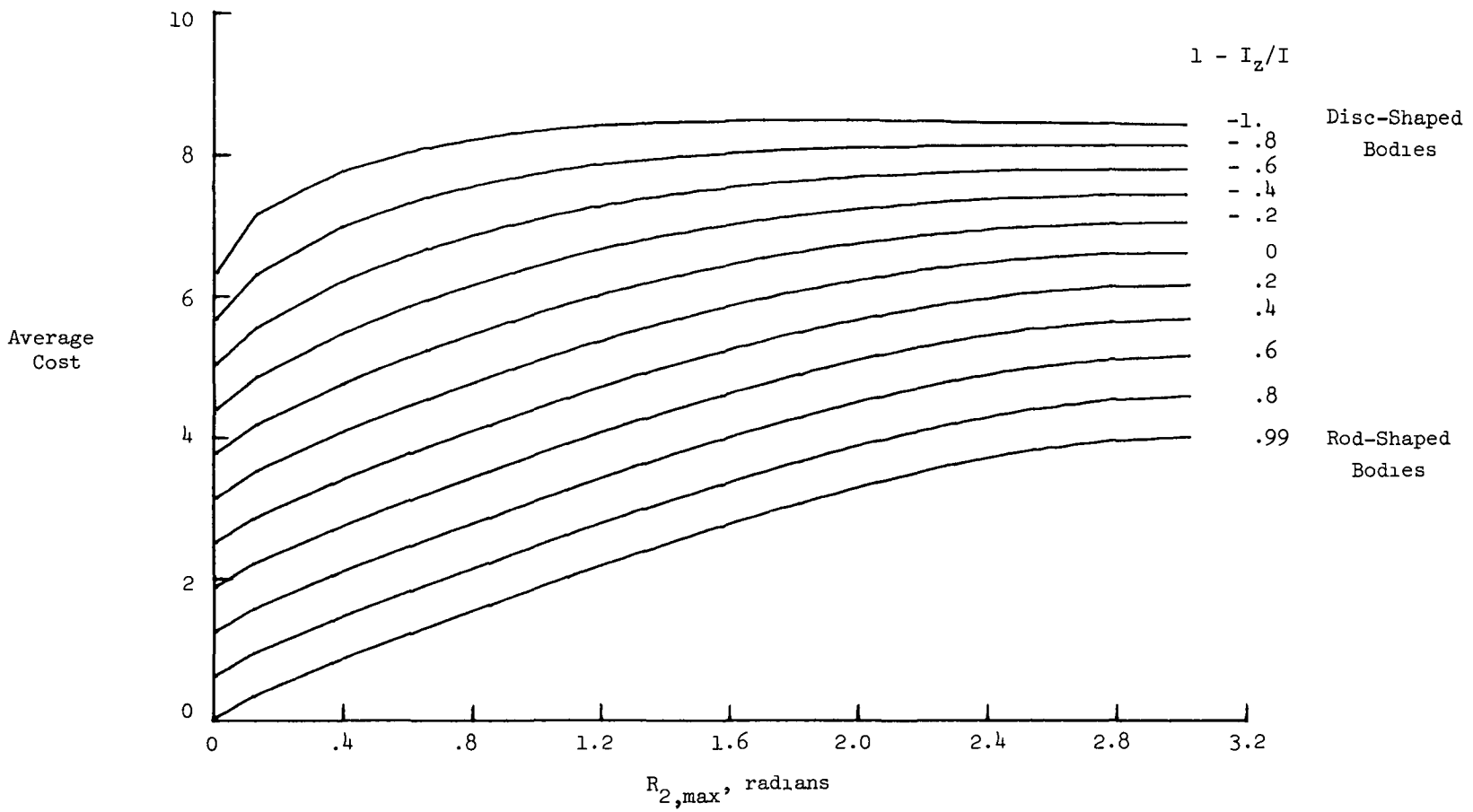


Figure 8.- Effect of maneuver range on average cost for reorientation over a range of $1 - I_z/I$ values for axisymmetric bodies.

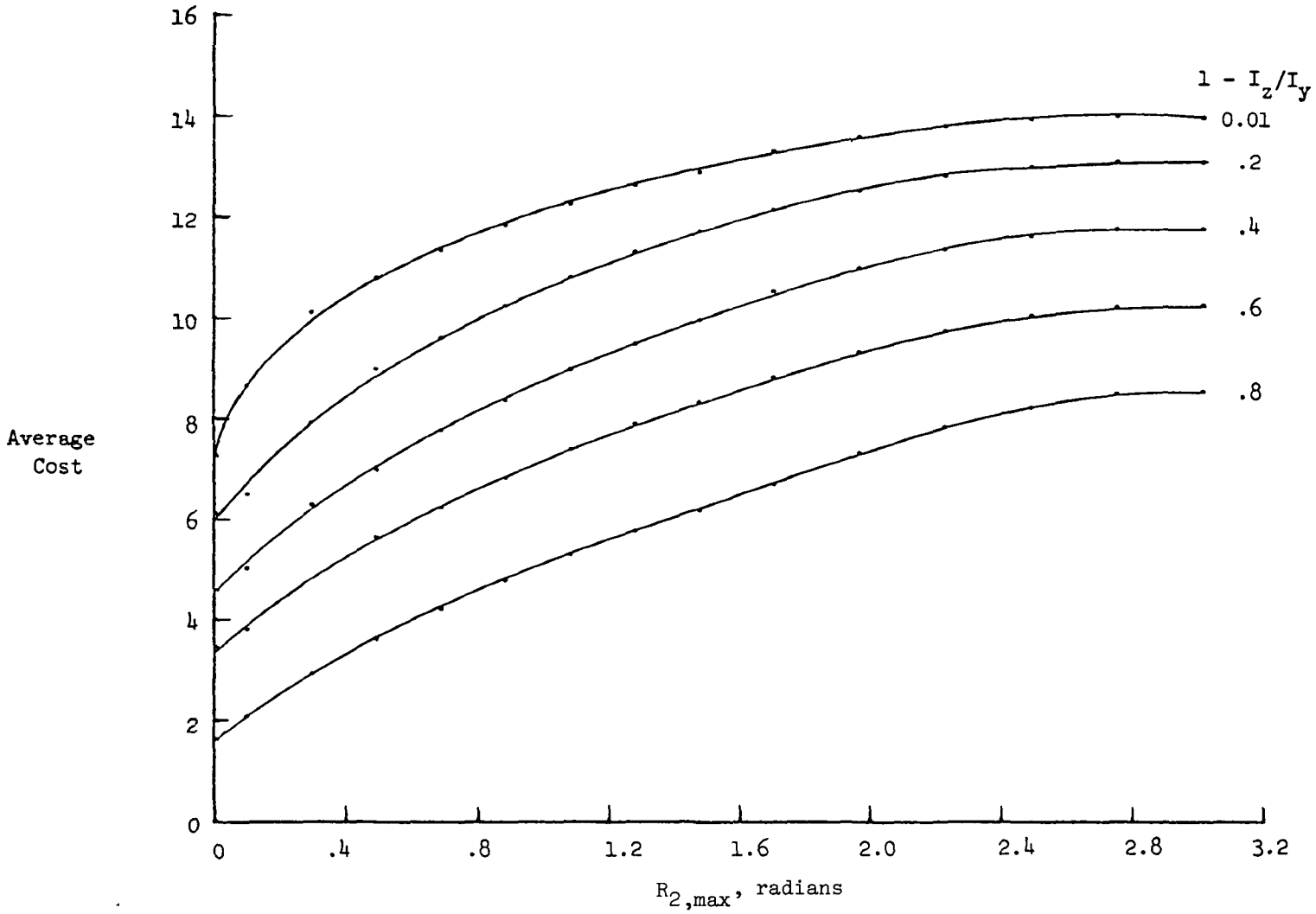


Figure 9.- Effect of maneuver range on average cost of reorientation for asymmetric bodies with $I_x/I_y = 1.2$.

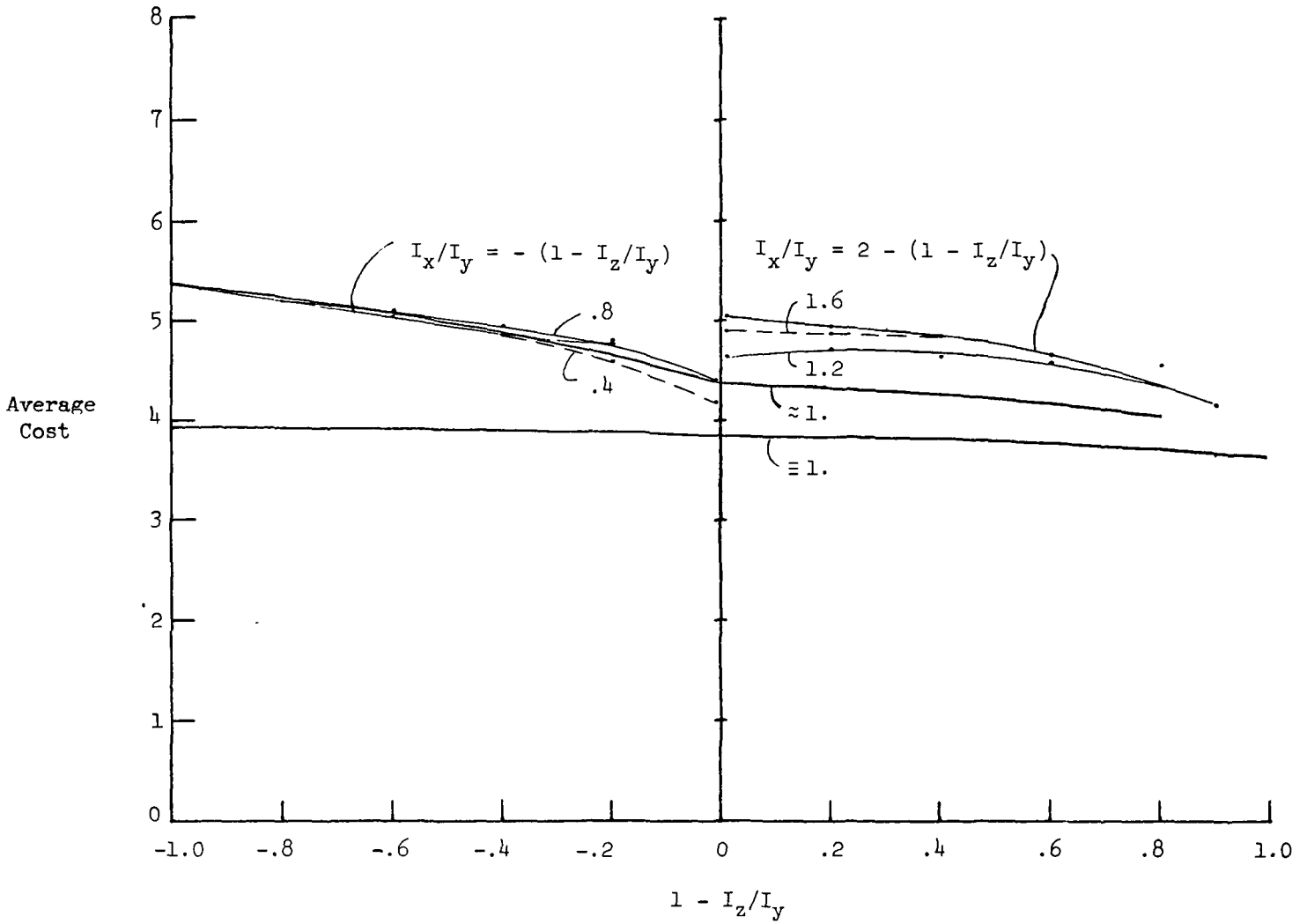


(a) Maneuver range = π radians.

Figure 10.- Effect of inertia distribution on average cost of spin-axis reorientation.

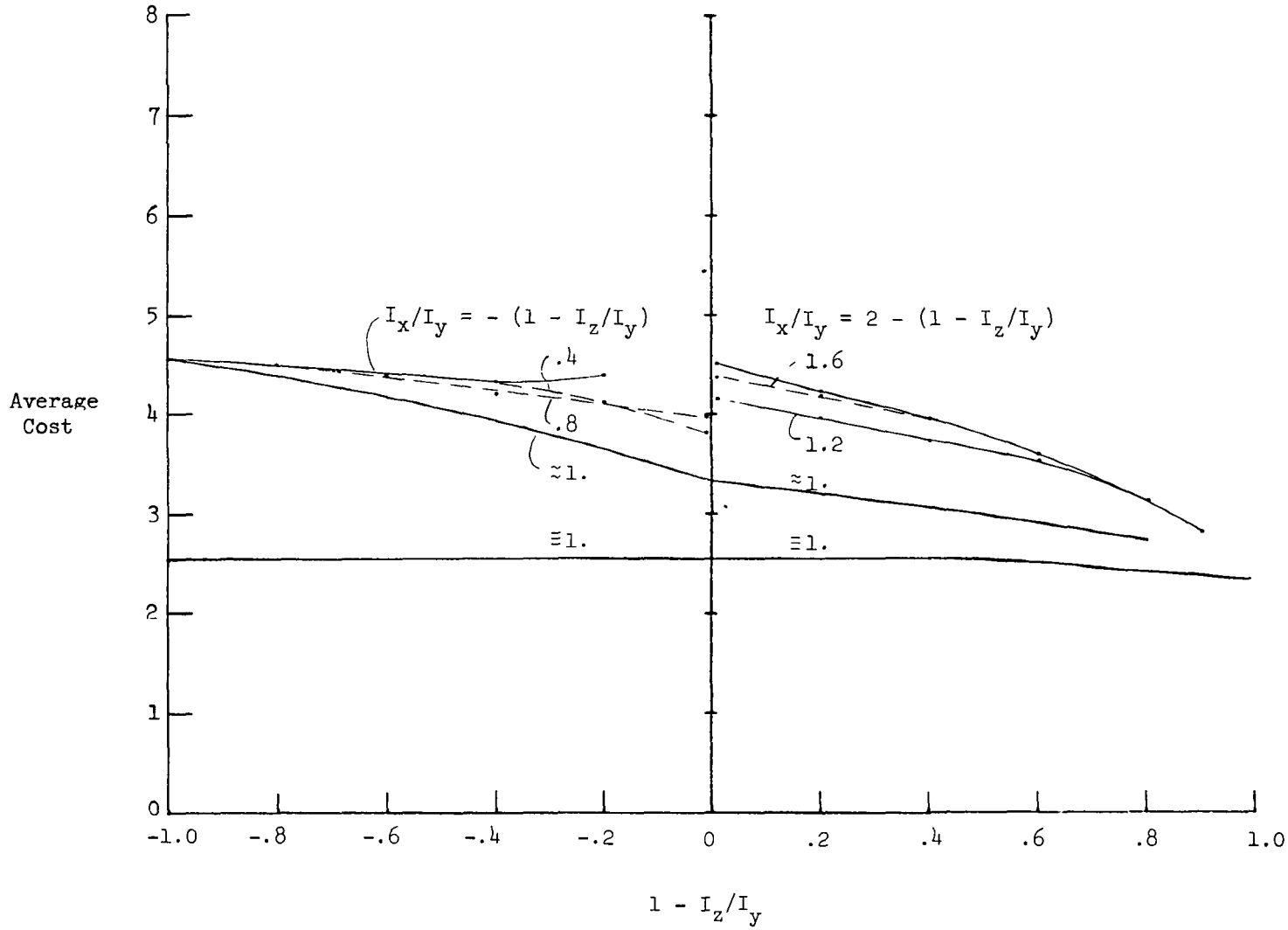


(b) Maneuver range = π/2 radians.

Figure 10.- Continued.

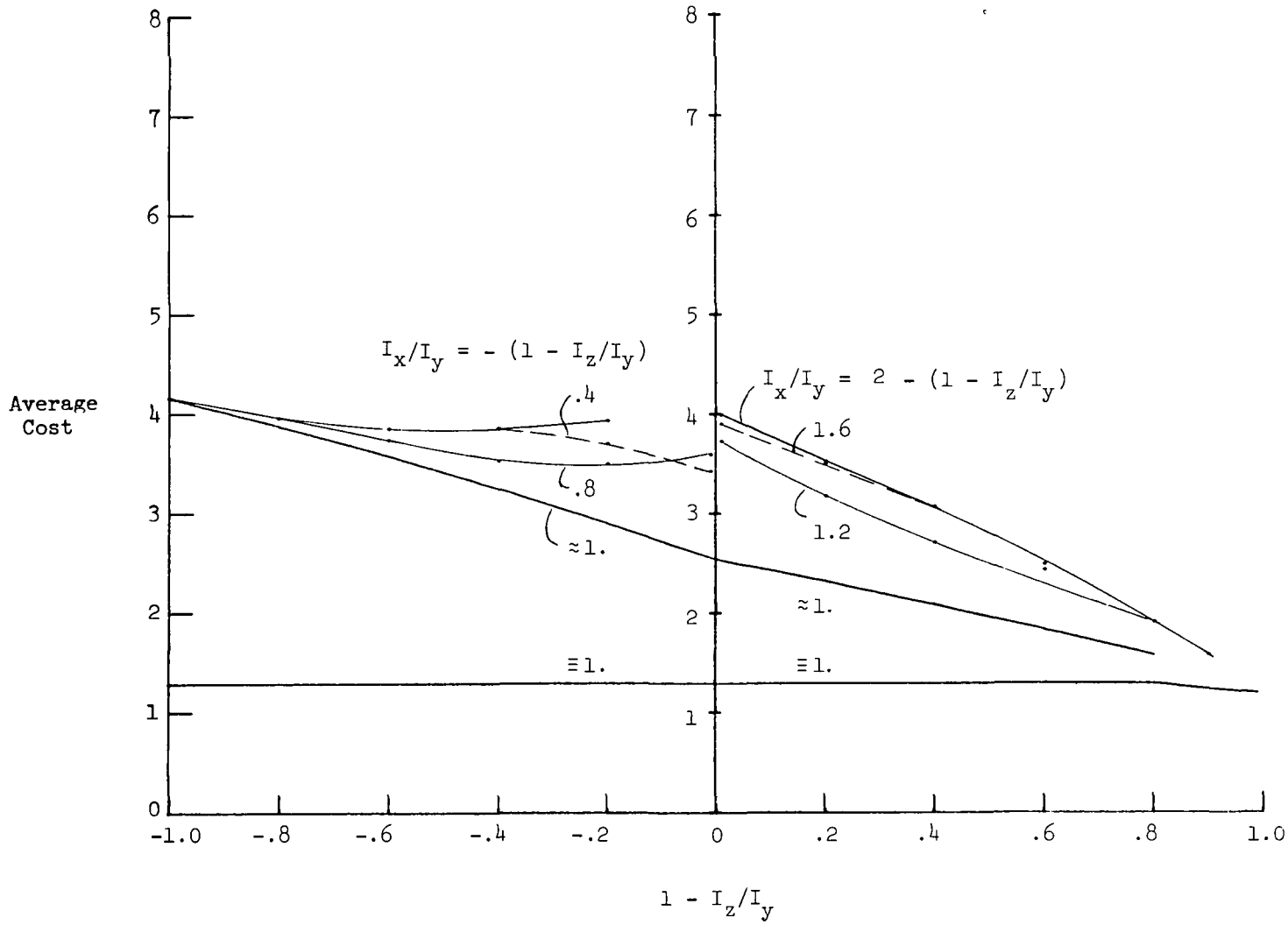


(c) Maneuver range = π/4 radians.

Figure 10.- Continued.

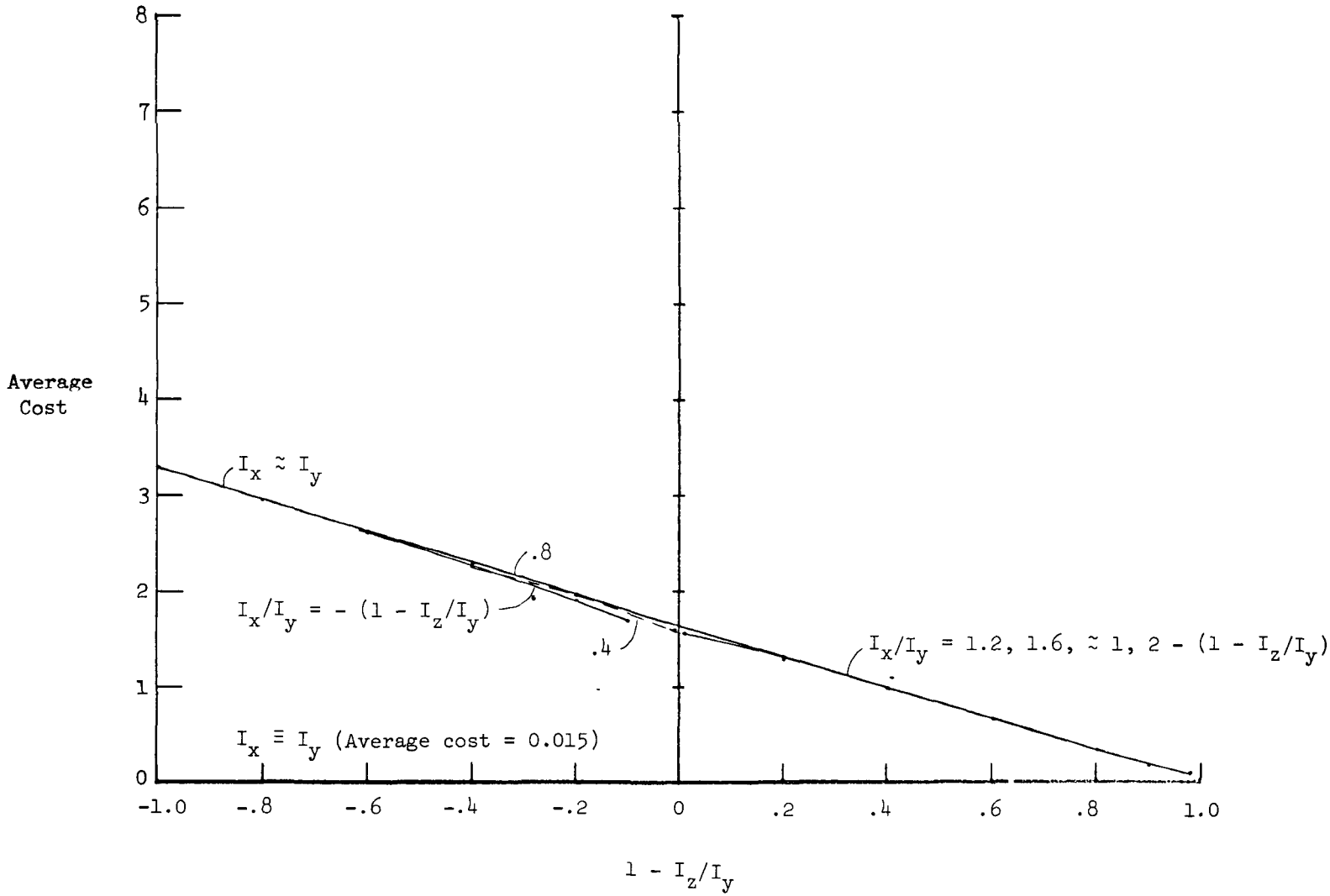


(d) Maneuver range = 0.00873 radian.

Figure 10.- Concluded.

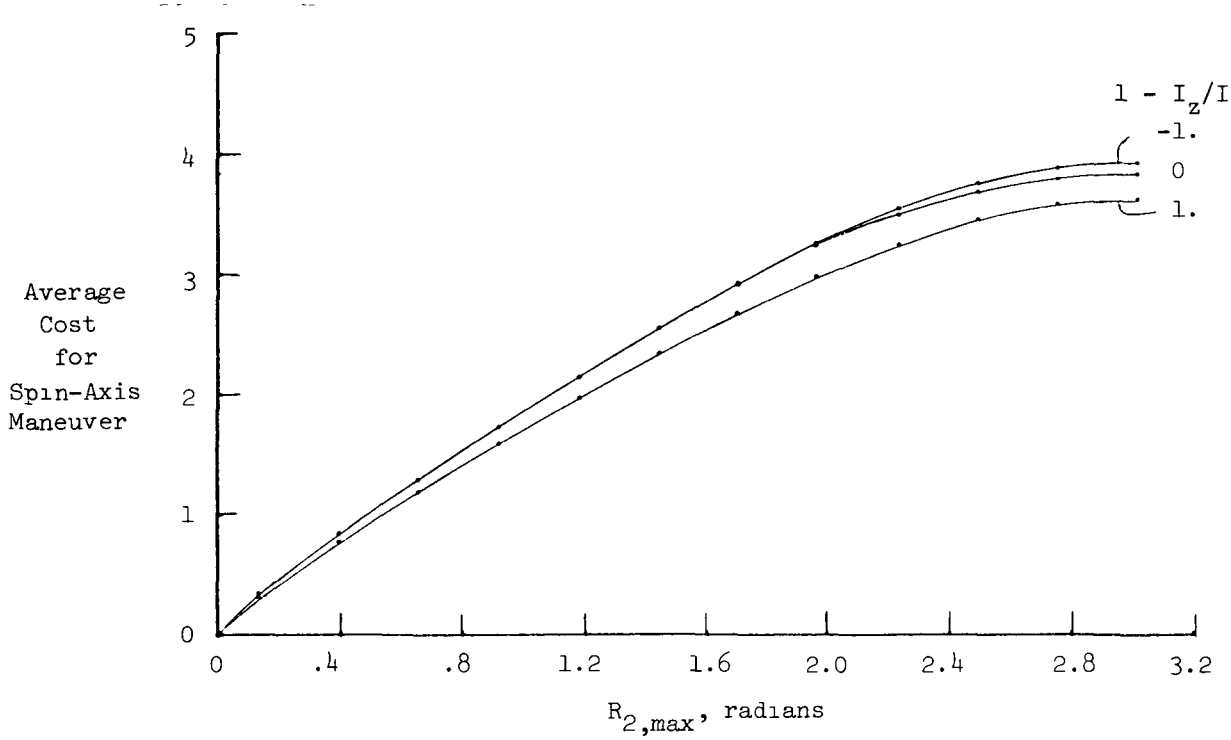


Figure 11.- Effect of maneuver range on cost of spin-axis reorientation for roll-symmetric bodies.

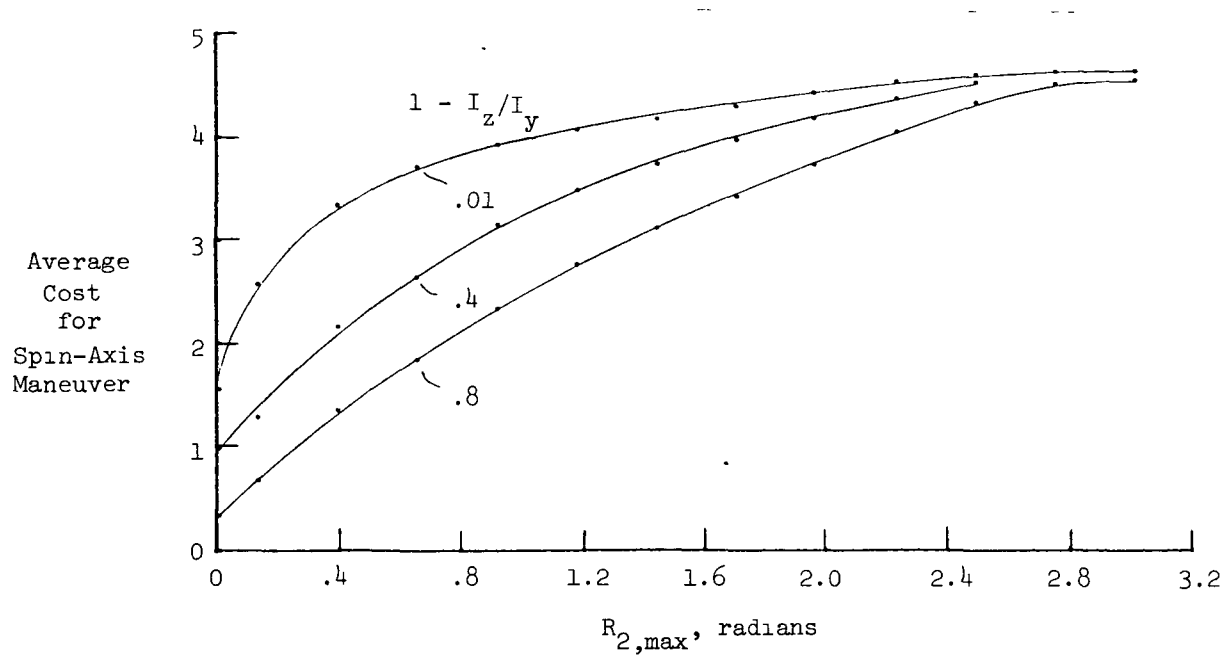


Figure 12.- Effect of maneuver range on cost of spin-axis reorientation for asymmetric bodies with $I_x/I_y = 1.2$.



NASA-Langley, 1977 L-11127

NATIONAL AERONAUTICS AND SPACE ADMINISTRATION
WASHINGTON, D C 20546

OFFICIAL BUSINESS
PENALTY FOR PRIVATE USE $300

THIRD-CLASS BULK RATE

POSTAGE AND FEES PAID
NATIONAL AERONAUTICS AND
SPACE ADMINISTRATION
451

U.S.MAIL

POSTMASTER If Undeliverable (Section 158 Postal Manual) Do Not Return

*"The aeronautical and space activities of the United States shall be conducted so as to contribute . . to the expansion of human knowledge of phenomena in the atmosphere and space The Administration shall provide for the widest practicable and appropriate dissemination of information concerning its activities and the results thereof."*

—NATIONAL AERONAUTICS AND SPACE ACT OF 1958

# NASA SCIENTIFIC AND TECHNICAL PUBLICATIONS

TECHNICAL REPORTS Scientific and technical information considered important, complete, and a lasting contribution to existing knowledge.

TECHNICAL NOTES Information less broad in scope but nevertheless of importance as a contribution to existing knowledge

TECHNICAL MEMORANDUMS Information receiving limited distribution because of preliminary data, security classification, or other reasons. Also includes conference proceedings with either limited or unlimited distribution.

CONTRACTOR REPORTS Scientific and technical information generated under a NASA contract or grant and considered an important contribution to existing knowledge

TECHNICAL TRANSLATIONS Information published in a foreign language considered to merit NASA distribution in English

SPECIAL PUBLICATIONS Information derived from or of value to NASA activities. Publications include final reports of major projects, monographs, data compilations, handbooks, sourcebooks, and special bibliographies

TECHNOLOGY UTILIZATION PUBLICATIONS· Information on technology used by NASA that may be of particular interest in commercial and other non-aerospace applications Publications include Tech Briefs, Technology Utilization Reports and Technology Surveys.

***Details on the availability of these publications may be obtained from:***

**SCIENTIFIC AND TECHNICAL INFORMATION OFFICE**

**NATIONAL AERONAUTICS AND SPACE ADMINISTRATION**

**Washington, D.C. 20546**